



On the outflow of dense water from the Weddell and Ross Seas in OCCAM model

R. Kerr^{1,2}, K. J. Heywood³, M. M. Mata^{1,2}, and C. A. E. Garcia¹

¹Laboratório de Estudos dos Oceanos e Clima, Instituto de Oceanografia, Universidade Federal do Rio Grande (FURG), Rio Grande, RS, 96203-900, Brazil

²Instituto Nacional de Ciência e Tecnologia da Criosfera (INCT-CRIOSFERA), RS, Brazil

³School of Environmental Sciences, University of East Anglia (UEA), Norwich, NR4 7TJ, UK

Correspondence to: R. Kerr (rodrigokerr@furg.br)

Received: 21 June 2011 – Published in Ocean Sci. Discuss.: 11 July 2011

Revised: 27 April 2012 – Accepted: 11 May 2012 – Published: 14 June 2012

Abstract. We describe the seasonal and interannual variability of volume transports in the Weddell and Ross Seas using the 1/12° 20-yr simulation of the OCCAM global ocean general circulation model. The average simulated full-depth cumulative volume transports were 28.5 ± 2.9 Sv ($1 \text{ Sv} \equiv 10^6 \text{ m}^3 \text{ s}^{-1}$) and 13.4 ± 5.2 Sv, across the main export regions of the Weddell and Ross Seas, respectively. The values of mean outflow of Antarctic Bottom Water (AABW) (defined by neutral density $\gamma^n \geq 28.27 \text{ kg m}^{-3}$) from the Weddell and Ross Seas of 10.6 ± 3.1 Sv and 0.5 ± 0.7 Sv, respectively, agree with the range reported in historical observational studies. The export of Weddell Sea dense water in OCCAM is primarily determined by the strength of the Weddell Gyre. Variability in AABW export is predominantly at periods of ~ 1 yr and 2–4 yr.

into deep and bottom ocean layers until they reach their density equilibrium in the water column. The densest water that fills the global ocean basins has its main sources in the regional seas around the Antarctic continent and is referred to as Antarctic Bottom Water (AABW) after leaving the source regions (Orsi et al., 1999).

AABW is a mixture of different source water masses with origins both in the coastal and deep ocean. Its properties depend on several complex physical coupled ocean-atmosphere-cryosphere processes that occur during its formation, including sea ice growth and brine rejection, opening of coastal polynyas, melting under deep ice shelves, deep convection, and entrainment of overlying or surrounding waters (Gill, 1973; Carmack and Foster, 1975; Foldvik et al., 1985; Nicholls et al., 2009). The Weddell and Ross Seas (Fig. 1) have broad (~ 400 km) and deep (~ 400 m) continental shelves that facilitate some of the processes listed above. AABW is produced at the Antarctic continental margins through mixture of shelf waters near the freezing point (High Salinity Shelf Water – HSSW, and Ice Shelf Water – ISW) with relatively warm and salty intermediate waters (Warm Deep Water – WDW, Modified WDW – MWDW, and Circumpolar Deep Water – CDW, Modified CDW – MCDW). Figure 2 indicates these water masses in potential temperature-salinity (θ/S) space.

During the last decade, several studies have highlighted the variability and trends in the physical properties of AABW source water masses. For example, a long-term freshening of shelf water masses of both the Weddell and Ross Seas has been observed (Jacobs et al., 2002; Jacobs and Giulivi,

1 Introduction

During the fourth International Polar Year (IPY; 2007–2009), the scientific community focused on better understanding the interactions between ocean, atmosphere, and cryosphere, and the role and susceptibility of polar regions in a climate change scenario. The *Synoptic Antarctic Shelf-Slope Interactions Study* (SASSI) project coordinated by the International Antarctic Zone Programme (iAnZone) brought a coordinated international sampling effort around the Antarctic margins (i.e. the zone around the continental shelf-break) during the IPY. The importance of this ocean boundary region between coastal and deep zones is related to dense waters cascading

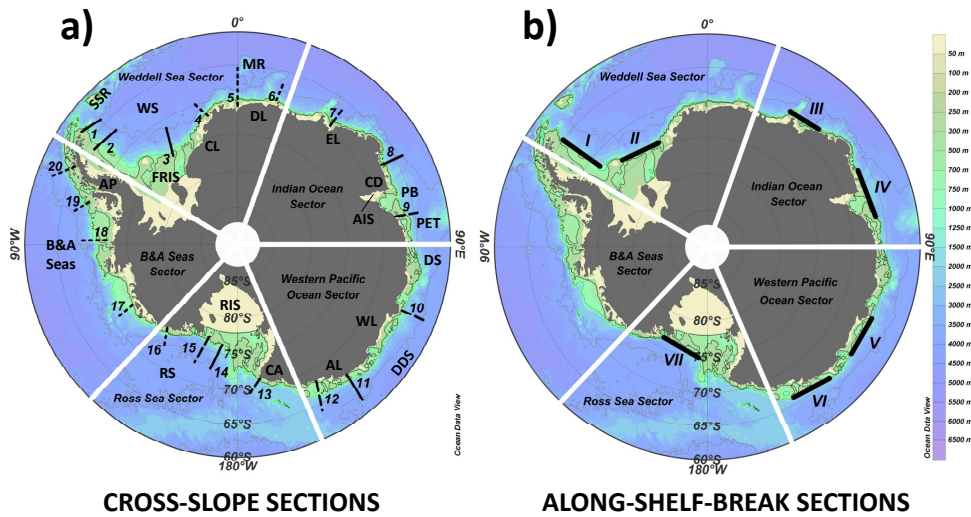


Fig. 1. Southern Ocean sectors with (a) cross-slope sections and (b) along-shelf-break sections. The thin black, green, and grey lines are the 500 m, 1000 m and 4000 m isobaths. The black thick, dashed and dotted lines in (a) denote regions of active, passive and null Antarctic Bottom Water downslope flow, respectively. Adelie Land Coast = AL, Amery Ice Shelf = AIS, Antarctic Peninsula = AP, Bellingshausen and Amundsen = B&A, Cape Adare = CA, Cape Darnley = CD, Coats Land = CL, Dumont d'Urville Sea = DDS, Dronning Maud Land = DL, Davis Sea = DS, Enderby Land Coast = EL, Filchner-Ronne Ice Shelf = FRIS, Maud Rise = MR, Prydz Bay = PB, Princess Elizabeth Trough = PET, Ross Ice Shelf = RIS, Ross Sea = RS, South Scotia Ridge = SSR, Wilkes Land Coast = WL, Weddell Sea = WS.

2010; Hellmer et al., 2011), but the causes of this freshening are still under debate (e.g. Assmann and Timmermann, 2005; Rignot and Jacobs, 2002). Hellmer et al. (2009) showed that decadal variability of the salinity of the southwestern Weddell Sea shelf water can be related to the Southern Annular Mode, which impacts both the ocean dynamics and sea ice processes in the Southern Ocean (Hall and Visbeck, 2002) and, consequently, the AABW contribution to the deep ocean (Kerr et al., 2009a).

At the same time, changes in the intermediate depth source waters of AABW have been reported for recent decades. Gille (2002) showed that Southern Ocean waters between 700 m and 1000 m depth had a warming of about $+0.01\text{ }^{\circ}\text{C yr}^{-1}$ between the 1950s and 1990s. A similar warming ($\sim 0.012\text{ }^{\circ}\text{C yr}^{-1}$) was reported for the WDW inflow to the Weddell Sea during the 1975–2000 period (Robertson et al., 2002). Smedsrud (2005) reported WDW warming near the Greenwich Meridian from 1977 to 2001, while Fahrbach et al. (2004) showed evidence that this 40-yr warming period could have reversed after 1998. Alternating periods of WDW cooling and warming were already reported by Gordon (1982) during the 1970s.

The changes in AABW source water masses are impacting the properties of the recently ventilated deep and bottom waters formed around the Antarctic continent (e.g. Aoki et al., 2005; Johnson, 2009; Ozaki et al., 2009). Kerr et al. (2009a) revealed that the Weddell Sea Bottom Water (WSBW) contribution to the total water mass mixture in the Weddell Basin exhibited a decrease of $\sim 20\%$ between the 1980s and the

1990s both near the Greenwich Meridian (1984–1998) and in the World Ocean Circulation Experiment (WOCE) SR4 repeat section (Fahrbach et al., 2004) near the tip of the Antarctic Peninsula (1989–1998). Aoki et al. (2005) indicated that bottom waters in the Antarctic-Australian Basin became cooler ($\sim 0.2\text{ }^{\circ}\text{C}$) and fresher (~ 0.03) over the period 1994 to 2003. Rintoul (2007) highlighted a faster AABW freshening between 1995 and 2005 than that observed between the late 1960s and the 1990s. Through analyses of historical hydrographic data, Azaneu et al. (2012) recently revealed that AABW in the Southern Ocean has become lighter throughout the last 50 years (1958–2010).

Our present study aims to better understand the seasonal and interannual variability of AABW volume transport around the Antarctic continent and export to the global oceans. Here, we focus our investigation on comparing the results from the Weddell and Ross Seas, two of the main areas of AABW production (Orsi et al., 1999). It is well known that synoptic and almost uninterrupted measurements over a long time period and throughout all seasons are required to perform time series analyses. However, historically observed subsurface Southern Ocean databases lack long records, are seasonally biased and suffer from scarcity of data in some areas of difficult access due to environmental conditions and/or logistic operations. Therefore, we used instead output from the high spatial resolution $1/12^{\circ}$ global eddy-resolving version of the Ocean Circulation and Climate Advanced Modelling (OCCAM) model (Coward and de Cuevas, 2005).

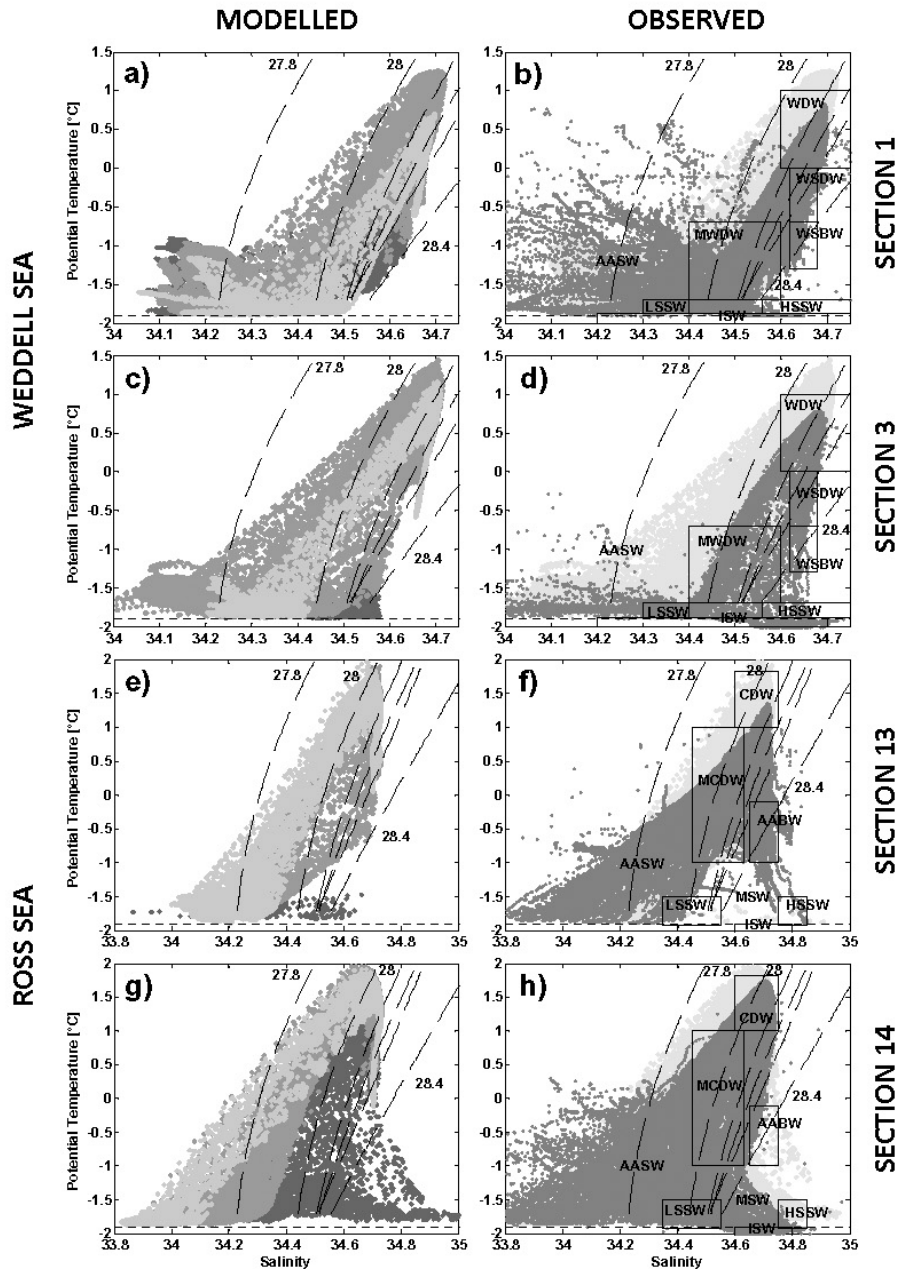


Fig. 2. (a–d) Weddell and (e–h) Ross Seas OCCAM monthly average (left column) and (right column) observed potential temperature/salinity (θ/S) diagrams. Colours in the left column indicate continental shelf (dark grey), continental slope (grey), and deep ocean (light grey). Colours in the right column indicate OCCAM simulation (light grey) and observations (dark grey). Dashed lines are neutral densities of 27.8, 28, 28.1, 28.2, 28.27, 28.40 kg m^{-3} respectively. The dotted line is the freezing point temperature. See the text for water mass definitions. Antarctic Surface Water = AASW, High Salinity Shelf Water = HSSW, Ice Shelf Water = ISW, Low Salinity Shelf Water = LSSW, Circumpolar Deep Water = CDW, Warm Deep Water = WDW, Modified CDW = MCDW, Modified WDW = MWDW, Modified Shelf Water = MSW, Antarctic Bottom Water = AABW, Weddell Sea Deep Water = WSDW, and Weddell Sea Bottom Water = WSBW.

2 Model description and forcing

OCCAM is a global ocean general circulation model (OGCM) (Coward and de Cuevas, 2005) coupled with a dynamic-thermodynamic sea ice model (Aksenov, 2002).

Such a sea ice model is essential to reproduce AABW properties in OGCMs (Kerr et al., 2009b), because both dynamic and thermodynamic sea ice processes play significant roles in Southern Ocean climate variability and bottom water formation (Jacobs and Comiso, 1989; Venegas and Drinkwater,

2001). However, cryosphere processes related to ice shelves, icebergs and ice sheet runoff are not included in the model. The model has 66 levels in the vertical, whose thickness increases from 5 m at the surface to 205 m for the deepest layer. The bathymetry is constructed from Smith and Sandwell (1997) and Digital Bathymetry Database 5' (DBDB5, 1983), with some depth sills manually corrected.

The OCCAM model was run at the National Oceanographic Centre, Southampton, UK. We use the monthly output from the OCCAM 1/12° simulation called “run 401” (Coward and de Cuevas, 2005), extracted from the OCCAM data selector website (<http://www.noc.soton.ac.uk/JRD/OCCAM/EMODS/>). The output variables used here are potential temperature, salinity, and zonal and meridional velocity. The run was forced using 6 hourly winds and heat fluxes from the National Centers for Environmental Prediction (NCEP) reanalysis data (Kalnay et al., 1996; Large et al., 1997) and was initialized using WOCE climatology (Gouretski and Jancke, 1996) for potential temperature and salinity with additional data for the Arctic Ocean. The initial condition to run the sea ice model in the Southern Ocean was set to 1.50 m thickness of sea ice and 0.15 m snow in all cells south of 65.25° S with an ice concentration of 99 % in each affected grid cell. The simulation ran for 20 yr spanning from 1985 to 2004, although our analysis excludes the first 4 yr, because this period includes the model spin-up phase.

A detailed assessment of the OCCAM 1/12° simulation regarding the representation of physical properties in the Weddell Sea was discussed by Renner et al. (2009). They highlighted that the choice of model must be made carefully and according to the purpose of the study. They demonstrated that OCCAM 1/12° simulation (hereafter referred to as OCCAM only) is a good choice to analyse deep water masses. Here, we extend their analysis by providing a validation of the model AABW volume transport time series (see Sect. 5.1) describing the seasonal and interannual variability. Hereafter the reader is directed to Fig. 1 for all regional oceanic and topographic locations cited in the text.

3 Model sections and bottom-layer definition

3.1 Cross-slope hydrographic sections

Twenty cross-slope hydrographic sections around the Antarctic continent (Fig. 1a) were primarily chosen based on the work of Baines and Condie (1998) to investigate the model circumpolar AABW flow along the Antarctic continental margin. They classified the Antarctic continental margins as active, passive or null in terms of AABW downslope flow. Here, we focus the discussion on four continental shelf and slope cross-sections selected in the Weddell and Ross Seas to investigate the AABW response to shelf and intermediate depth source water variability. These sections, described below, were chosen because they are sites of AABW

downslope or alongslope flow, and also because of the availability of historical data nearby.

In the Weddell Sea the main sections discussed are (i) Sect. 1 – the main outflow route of bottom water export (Naveira Garabato et al., 2002; Franco et al., 2007), coincident with the western part of the WOCE SR4 repeat section (Fahrbach et al., 2004), and (ii) Sect. 3 – the southern continental shelf near the Filchner-Ronne Ice Shelf that is known as a region of AABW production (Foldvik et al., 1985; Nicholls et al., 2009). In the Ross Sea the sections analysed are (i) Sect. 13 – the bottom water outflow area near Cape Adare, which is an area intensively studied through the US Cross-Slope Exchanges at the Antarctic Slope Front (AnSlope) and the Italian Climatic Long-term Interaction for the Mass balance in Antarctica (CLIMA) programs (Gordon et al., 2009), and (ii) Sect. 14 – close to the west branch of the Ross Sea cyclonic gyre, which is indicated as an export area of the less dense variety of Ross Sea Bottom Water (RSBW; Ozaki et al., 2009). We need to bear in mind that these cross-slope sections refer to transports of recirculating and new AABW varieties in the Weddell and Ross Seas (i.e. transports along the continental slope). Sections 1 and 13 are respectively the main zones in the Weddell and Ross Seas of AABW export to the global oceans. All sections spanned from ~500 m to 4000 m deep, except for the Ross Sea cross-slope section 13 that extends only to 3000 m because of the complex bathymetry surrounding the area.

3.2 Along-shelf-break hydrographic sections

To explore the dense bottom water that is leaving the continental shelf and cascading down the slope in the model, seven along-shelf-break hydrographic sections around the 1000 m isobath (Fig. 1b) were defined according to the AABW source areas compiled by Hay (1993), which are primarily based on the Killworth (1977) study. The along-shelf-break section IV was added because of the recent reports of AABW formation in this area (e.g. Wong et al., 1998; Yabuki et al., 2006). These sections were defined to quantify the dense water mass exported across the continental shelf-break. The definitions in density space of deep and bottom water mass layers used here for both cross-slope and along-shelf-break sections are explained in Sect. 3.3.

3.3 Bottom-layer definition

In this study we do not attempt to distinguish between the regional differences of deep and bottom water masses around the Southern Ocean, since we wish to use a consistent definition for all regions. Hereafter, we define the *bottom-layer* as the part of the water column denser than neutral density (γ^n ; Jackett and McDougall, 1997) of 28.27 kg m^{-3} , in accordance with the definition of AABW given by Orsi et al. (1999). This layer encloses all AABW regional varieties in the Southern Ocean despite the differences in their

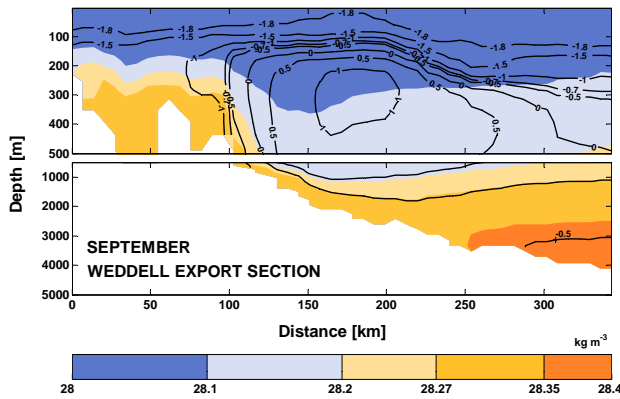


Fig. 3. Weddell Sea cross-slope section 1 fields of (colour) neutral density in kg m^{-3} and (isolines) potential temperature in $^{\circ}\text{C}$ of OCCAM September climatology (1988–2004).

physical properties in each source area (Whitworth et al., 1998). In fact, the bottom-layer as defined here encloses the entire deep and bottom water mass with θ lower than 0°C in the continental slope and deep ocean. This can be clearly seen in OCCAM fields for the Weddell Sea cross-slope section 1 (Fig. 3; see for comparison the Southern Ocean Atlas of Orsi and Whitworth, 2004), where the September climatology is given as an example of the typical water mass structure. Moreover, OCCAM model reproduces well these bottom waters around the Antarctic continental margins, particularly in the Weddell Sea (Renner et al., 2009), Indian Ocean and inner Ross Sea sectors (see Sect. 4.1; Fig. 4).

4 Southern Ocean representation

4.1 OCCAM water masses representation

Figure 2 shows a comparison between observed and simulated θ/S diagrams of the main continental shelf and slope cross-sections that are analysed here. The observed thermohaline values were obtained from the World Ocean Database 2005 (WOD05; Boyer et al., 2006). In order to maximise the number of observations, we selected all conductivity-temperature-depth (CTD) data within 2° longitude (~ 100 km for cross-slope section 1 and ~ 70 km for all other sections) east and west of each section. Although ice shelf processes are not considered in OCCAM, which is evidenced by the lack of ISW representation in the model, dense water masses on the continental shelf are represented reasonably well in the sections (Fig. 2). The HSSW absence in some of the θ/S diagrams shown (e.g. Fig. 2a) is because only small fractions of the cross-slope sections lie over the continental shelf.

In order to quantify OCCAM’s performance in reproducing the observed hydrography in the Southern Ocean circum-polar cross-slope sections (Fig. 1a), we calculated some statistical variables (correlation and root-mean-square error –

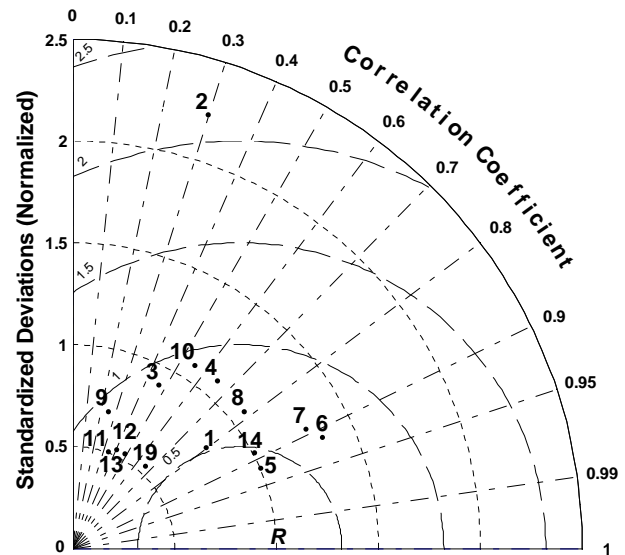


Fig. 4. Normalized pattern statistics showing differences between model and hydrographic observations of the neutral density bottom-layer ($\gamma^n \geq 28.27 \text{ kg m}^{-3}$) in each cross-slope section as indicated (Sections 1 to 14 & 19; see Fig. 1a). The short-dashed curves, long-dashed curves, and long-short-dash radii refer to normalised standard deviation, root-mean-square error and correlation, respectively. R = reference. WOD05 was the observed dataset used as reference (see the text for details).

RMSE) of observed and modelled variability of the thermohaline properties of the bottom-layer along the cross-slope sections around the Antarctic continent. The equations for the statistical variables are given by Taylor (2001) and the output displayed in a Taylor diagram (Fig. 4). We used the WOD05 dataset as the reference observations, marked by the point labelled “R”. Both normalised standard deviation ($\sigma_{\text{norm}} = \sigma_{\text{model}}/\sigma_{\text{obs}}$) and correlation coefficient are equal to 1 at the reference point R (Fig. 4). The better the correlation (radiating long-short dashed lines in Fig. 4) and the closer the standard deviation of the modelled data to the observations (short-dashed curves), the closer the corresponding model point will be to the reference point R. The lines of low RMSE values mark the best fit considering both the correlation and the variability pattern. This model-observation bottom-layer statistical comparison through the Taylor diagram (Taylor, 2001) supports the good representation of the modelled dense water masses seen in the θ/S diagrams (Figs. 2 and 4). This is particularly true for those regions with repeat observations and regular historical sampling (e.g. cross-slope sections 1, 5 and 14 in Fig. 1a). Not surprisingly, the hydrography of the regions with direct influence from permanent ice shelves (e.g. cross-slope sections 2, 3 and 9 in Fig. 1a) is poorly represented by the model. However, the model-observation comparison of these sections may also be influenced by lack of observations near the permanent ice shelves. In general,

the bottom-layer in the model for the western Pacific Ocean and Bellingshausen and Amundsen (B&A) Seas sectors (e.g. cross-slope sections 10, 11–13 and 19 in Fig. 1a) does not satisfactorily represent the observed bottom-layer properties.

Intermediate waters, with γ^n between 28.0 kg m^{-3} and 28.27 kg m^{-3} , are warmer and saltier than observations by $\sim 0.5^\circ\text{C}$ and ~ 0.03 , respectively, in all sections (Fig. 2). Despite the slight differences in θ and S absolute values, the model shows a good representation of water masses in the Weddell and Ross Seas continental margins, as earlier reported for the northwestern Weddell Sea by Renner et al. (2009). OCCAM preserves the observed general θ/S shape for both coastal and deep ocean in the Antarctic continental margins (Figs. 2 and 4), which provides a high degree of confidence to perform subsequent analysis of the model time series. A complete circumpolar overview of OCCAM water mass structure and hydrographic representation in the Southern Ocean is given by Kerr (2010).

4.2 Modelled AABW source layer depth

Two depth ranges were chosen from OCCAM to represent the AABW source water masses. We represent the shelf/surface layer (SL) as an average of the 4 model levels between 100 m and 150 m (levels 15–18) and the intermediate layer (IL) as an average of the 4 model levels between 400 m and 600 m (levels 28–31). The SL defined here encompasses both the shelf water masses in the Antarctic coastal regime and the mixture of waters at the continental slope, such as MWDW in the Weddell Sea, which is an important source for AABW formation (Foster and Carmack, 1977). In the open ocean, the SL represents the Antarctic surface water masses. The IL encompasses the densest shelf waters present on the broad western and southwestern continental shelves as well as the cores of intermediate depth source water that reach the continental slope (e.g. WDW θ_{max} is found around 500 m in the Weddell Sea; Orsi et al., 1993).

Averaged fields of potential temperature and salinity in the SL and IL are presented in Fig. 5 for the entire OCCAM period (1988–2004). The SL temperature is around -1.5°C in deep ocean and coastal regimes (Fig. 5a), characterising the winter water in the oceanic waters (i.e. a remnant of the deep winter mixed layer) and the shelf waters, respectively. The temperature slightly increases, but remains below 0°C , along the continental margin of the Weddell and Ross Seas (Fig. 5a), caused by mixing of shelf waters with intermediate waters (i.e. WDW or CDW) upwelled onto the shelves. Typical high salinity of the Weddell and Ross Seas shelf waters is observed in the Antarctic coastal regime of the model. The highest salinity plume (e.g. Gordon et al., 2004) of water from the western Ross Sea continental shelf is advected westward to $\sim 90^\circ\text{E}$ in the Davis Sea. CDW upwelling also contributes to the high salinity values simulated in the western Pacific Ocean sector (Fig. 5b). The increasing influence of mixing with WDW is noted in the Weddell Sea with in-

creasing salinity from $\sim 20^\circ\text{E}$ to near the coast of Enderby Land, following the Weddell Gyre circulation (Fig. 5b).

Values of θ in the IL are around surface freezing point ($< -1.5^\circ\text{C}$) near the Antarctic coast (Fig. 5c), slightly increasing offshore to $\sim 0^\circ\text{C}$. In open ocean areas, relatively warm CDW ($> 1^\circ\text{C}$) is seen in the Indian Ocean, western Pacific Ocean, Ross Sea, and B&A Seas sectors (Figs. 1 and 5). In the Weddell Sea, CDW cools through mixing with surrounding cooler waters as it enters in the Weddell Gyre, marked by WDW temperatures between 0°C and 0.5°C (Fig. 5c). The salinity field depicted in Fig. 5d shows most clearly the influence of CDW or WDW within the Ross and Weddell Seas. The model potential temperature and salinity fields at AABW source layers reveal that open ocean SL and IL waters are saltier and colder in the Weddell Sea, respectively, than in the Ross Sea, as has been noted previously by Orsi and Whitworth (2004).

5 Modelled AABW volume transport

5.1 Validation of the model AABW volume transport time series

To assess whether the bottom-layer volume transport time series are realistic, we compare the bottom-layer volume transport simulated by OCCAM in the Weddell Sea cross-slope section 1 (Fig. 1a) with previous observational studies in the same area carried out by Fahrbach et al. (1995) and Fahrbach et al. (2001), hereafter referred to as F95 and F01, respectively. The periods covered by the F95 and F01 analyses span between 1989–1993 and 1989–1998 respectively, and are included in the OCCAM-simulated period. The absolute values of observational and modelled bottom-layer volume transport differ, because different bottom-layer definitions are used (i.e. we include both AABW varieties found in the Weddell Sea); however, the two time series show the same temporal variability (Fig. 6). The OCCAM-simulated bottom-layer volume transport corresponds well with the observational studies both on interannual (Fig. 6a; $r = 0.53$; $p = 0.10$; $N = 10$) and monthly cycles (Fig. 6b; $r = 0.40$; $p = 0.05$; $N = 36$). In addition, the observed and modelled annual mean current velocity for the bottom-layer show similar magnitudes and temporal variability during the F01 observational period (Fig. 6c), with mean absolute bottom current velocity of $4.0 \pm 0.89 \text{ cm s}^{-1}$ (OCCAM) and $3.45 \pm 0.58 \text{ cm s}^{-1}$ (F01; see their Fig. 12a).

In addition, we compare OCCAM's bottom-layer in the Weddell Sea along-shelf-break (section I) with the full-depth volume transport in a similar area of the northwestern Weddell Sea (Fig. 6d), calculated by Muench and Gordon (1995; their Fig. 8). Some variations between the observed and simulated volume transport occur, probably due to spatial variability in this area and poor model resolution. Even so, OCCAM's volume transport captures the observed direction of

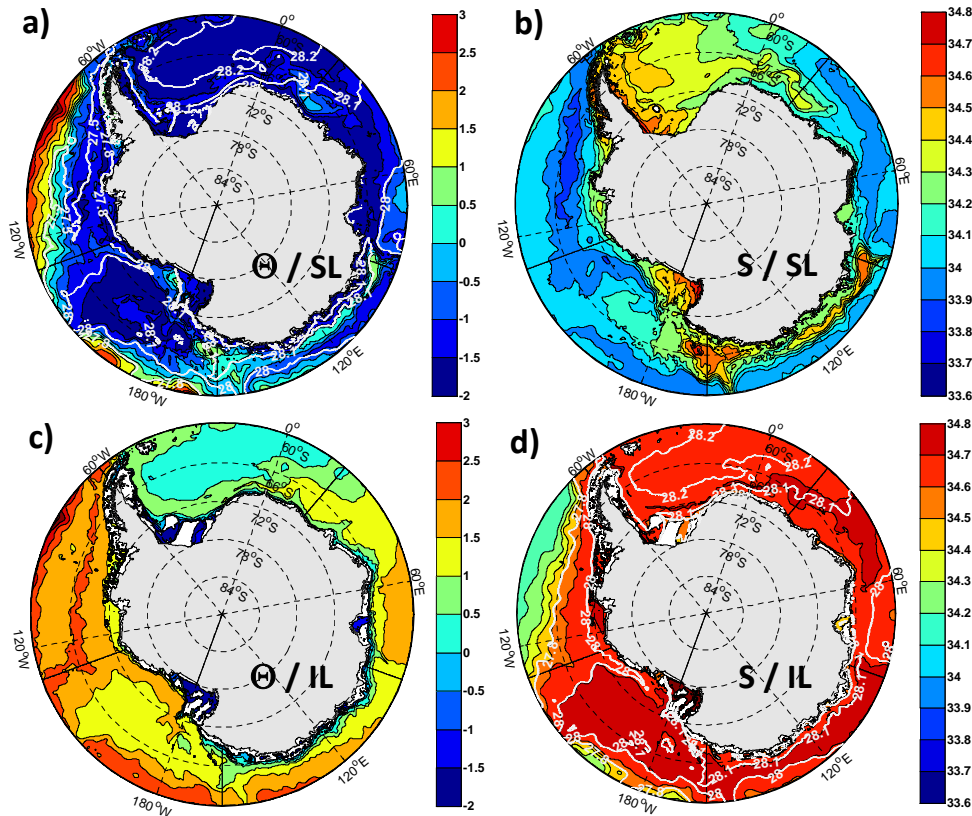


Fig. 5. OCCAM average field at (a and b) shelf/surface layer (SL) and (c and d) intermediate layer (IL) of (left) potential temperature (θ) in °C and (right) salinity (S). Neutral density surfaces (kg m^{-3}) are plotted in (a) and (d).

water mass flow (Fig. 6d). We are not aware of available time series for comparison of AABW volume transport in the Ross Sea.

5.2 Seasonal and interannual AABW volume transport variability

The mean full-depth volume transports, and their respective standard deviations, for the Weddell and Ross Sea cross-slope sections 1 and 13 during the 17-yr period of OCCAM simulation are respectively $28.5 \pm 2.9 \text{ Sv}$ ($1 \text{ Sv} \equiv 10^6 \text{ m}^3 \text{ s}^{-1}$) and $13.4 \pm 5.2 \text{ Sv}$, while for the cross-slope sections 3 and 14 the values are respectively $21.3 \pm 3.6 \text{ Sv}$ and $18.4 \pm 2.3 \text{ Sv}$ (Fig. 7). Positive transports denote northward/eastward. The error estimates quoted are the standard deviations of the monthly values over the 17-yr model run. The OCCAM-simulated transports are reasonable, compared with summertime observations and moored short time series for both Weddell (e.g. Fahrback et al., 1994; Muench and Gordon, 1995; Naveira Garabato et al., 2002) and Ross Seas (e.g. Reid, 1997; Chu and Fan, 2007).

Considering the bottom-layer, the average cumulative volume transports in OCCAM for Weddell and Ross Sea cross-slope sections 1 and 13 are $10.6 \pm 3.1 \text{ Sv}$ and $0.5 \pm 0.7 \text{ Sv}$ re-

spectively, while the cross-slope sections 3 and 14 transports are $3.1 \pm 0.9 \text{ Sv}$ and $0.5 \pm 0.4 \text{ Sv}$, respectively (Fig. 8). The export of Weddell Sea dense water in OCCAM is primarily determined by the strength of the Weddell Gyre, as the full-depth and bottom-layer transports vary synchronously (Figs. 7a, b and 8a, b) and are highly correlated ($r \geq 0.6$). One exception is the main export zone in the Ross Sea (section 13), which is not directly influenced by the Ross Gyre circulation implying that other physical processes are influencing AABW export. However, in the southern Ross Sea the strength of the Ross Gyre drives the bottom-layer export (Figs. 7d and 8d). Thus, OCCAM is primarily reproducing the gyres' variability due to their wind forcing, which agrees with recent observations (e.g. Jullion et al., 2010; Gordon et al., 2010; Meredith et al., 2011).

In general, the OCCAM mean bottom water export rates from Weddell and Ross Seas are well supported by observations. The OCCAM mean bottom-layer volume transport of $\sim 11 \text{ Sv}$ for the Weddell Sea cross-slope section 1 (Fig. 8a) is near the values of Weddell Sea Deep Water (WSDW) export over the South Scotia Ridge of $6.7 \pm 1.0 \text{ Sv}$ and $\sim 9 \text{ Sv}$ obtained, respectively, by Naveira Garabato et al. (2002) from LADCP data and by Franco et al. (2007) through a box

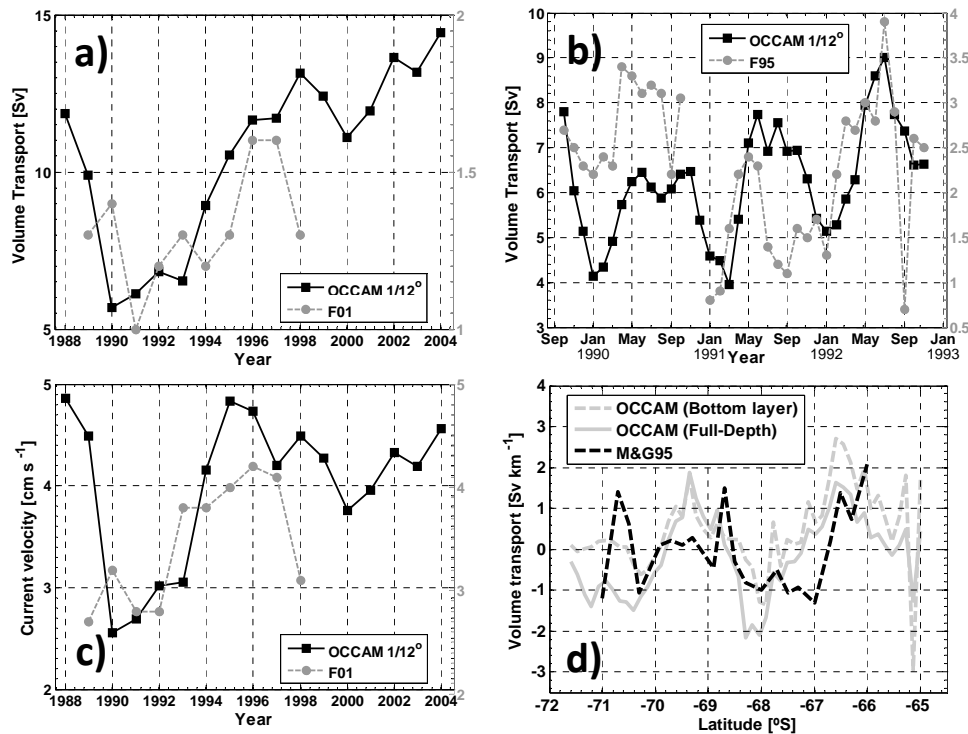


Fig. 6. Weddell Sea cross-slope section 1 bottom-layer volume transport (a) annual and (b) monthly average simulated by OCCAM (black line) and reported (grey line) by Fahrbach et al. (1995) = F95 and Fahrbach et al. (2001) = F01. (c) Same as described above, but for bottom-layer current velocity perpendicular to the bathymetry. (d) Northwestern Weddell Sea along-shelf-break section I full-depth and bottom volume transport vertically integrated and divided by the distance between the model grid points and observed hydrographic stations in a similar section to that observed by Muench and Gordon (1995) = M&G95 (see their Fig. 8). The values in (d) are normalized and represent the number of standard deviations from the overall mean.

inversion. In the Ross Sea, Whitworth and Orsi (2006) reported a transport of water colder than 0°C of 1.95 ± 1.85 Sv near the shelf break off Cape Adare. The mean bottom-layer transports of 0.5 ± 0.7 Sv and 0.5 ± 0.4 Sv simulated by OCCAM, respectively from the Ross Sea cross-slope sections 13 and 14 (Fig. 8c and d), are lower than the observed values, but their values are within the range of recent observations in the area cited above.

Jullion et al. (2010) showed by analysing AABW properties from repeat hydrography in eastern Drake Passage that wind stress variability over the Weddell Gyre leads to changes in AABW properties by approximately five months. The dynamical links between AABW export and surface variables were investigated here by performing a lagged correlation between zonal wind stress (estimated in a proxy area defined here as $60^{\circ}\text{--}65^{\circ}\text{S}$, $40^{\circ}\text{W--}20^{\circ}\text{E}$ where the wind drives the Weddell Gyre circulation) and the AABW export time series obtained from the cross-slope export section 1 in the Weddell Sea. Highest correlations are obtained with a five month lag and also around zero lag, both explaining $\sim 20\%$ ($r = 0.4$) of the observed variability. This five-month period is the same as previously reported by Jullion et al. (2010),

although our proxy latitude band for wind calculation is slightly different from theirs.

The simulated AABW volume transports for the Weddell Sea cross-slope sections 1 and 3 show a similar seasonal cycle, with the former showing the maximum volume transport lagging the latter by ~ 1 month (Fig. 9a). For cross-slope section 1, the maximum and minimum monthly mean transport of 12.2 ± 3.0 Sv and 8.6 ± 2.8 Sv were observed during June and January, respectively. For the cross-slope section 3, the maximum and minimum monthly mean transport of 4.0 ± 0.9 Sv and 2.2 ± 0.5 Sv occurred during May and January, respectively. Note that the values quoted here are actual values simulated by the model and not the values normalised by the monthly mean and standard deviation as shown in Fig. 9. The normalisation procedure was needed because of the difference in magnitude of volume transports in the sections (Fig. 8). Thus, the monthly mean transports of bottom water in the Weddell Sea show a maximum and minimum during early austral winter and summer, respectively, corroborating the results of F95 that showed the AABW outflow to be subject to a seasonal cycle with minimum temperatures and maximum velocities in early austral winter. In the Weddell Sea main export zone, there is an insignificant

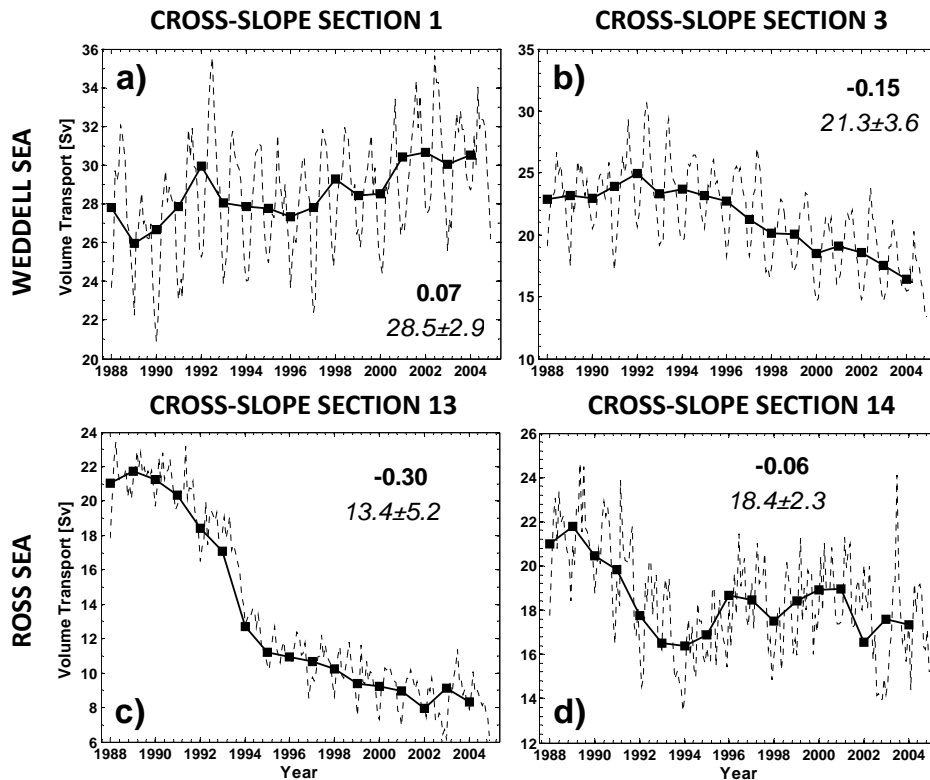


Fig. 7. Monthly (dashed line) and annual (full line) average of OCCAM full-depth cumulative volume transport for (a and b) Weddell and (c and d) Ross Seas cross-slope sections as indicated. Bold and italic annotations show respectively the decadal linear trend (Sv decade^{-1}) and the average and standard deviation for the entire period.

lag of approximately one month in the model seasonal cycle (Fig. 9a) compared with the results reported by F01, which showed maximum and minimum transport in May and December.

The seasonal cycles of bottom-layer volume transport in the Ross Sea for the cross-slope sections 13 and 14 are presented in Fig. 9b. The Ross Sea main export zone shows maximum and minimum monthly mean transports of $1.0 \pm 1.1 \text{ Sv}$ and $0.06 \pm 0.1 \text{ Sv}$ occurring during June and December, respectively, the same months as in the Weddell Sea. Inside the Ross Sea the cross-slope section 14 shows a semi-annual cycle with maxima in March–May and July–September and minima in June–July and December. The maximum and minimum monthly mean transports of $0.7 \pm 0.5 \text{ Sv}$ and $0.1 \pm 0.3 \text{ Sv}$ occurred in May and December respectively. Semi-annual cycles in current measurements and circulation strength have been observed in the Ross Gyre, as highlighted by Assmann et al. (2003) and references cited therein. There were no significant differences in the seasonal cycle of bottom-layer volume transport from cross-slope sections 2, 4, 15, and an alternative section chosen between cross-slope sections 12 and 13 (Fig. 9). These results support the robustness of the cross-slope sections chosen to rep-

resent the AABW volume transport variability of the whole regional area of the Weddell and Ross Seas.

Wavelet analysis of the detrended bottom-layer monthly volume transport time series reveals both the dominant modes of bottom-layer variability and how those modes vary in time (Fig. 10). In general, the dominant period of AABW volume transport variability is 1 yr due to seasonal changes in the wind-driven gyres (Fig. 11). However, the annual cycle is absent up to 1995 (see also Fig. 8c) for the Ross Sea cross-slope section 13, while in the Weddell Sea the annual cycle is significant through the whole time of the simulation. The wavelet analysis also highlights a significant periodicity of 2–4 yr for the AABW volume transport of the cross-slope section 1 (Fig. 10a) in the Weddell Sea, which is also present in the wind field over the Weddell Sea sector (Fig. 11), although not significant and continuous throughout the time series. For the Ross Sea cross-slope section 14 (not shown), low energy is associated with the variability of bottom water export. This low energy can be related to model deficiencies in reproducing the process of AABW spilling across the shelf-break of the Ross Sea, probably due to resolution issues (discussed in Sect. 5.3).

Venegas and Drinkwater (2001) found that sea ice concentration, sea ice drift and sea level pressure showed

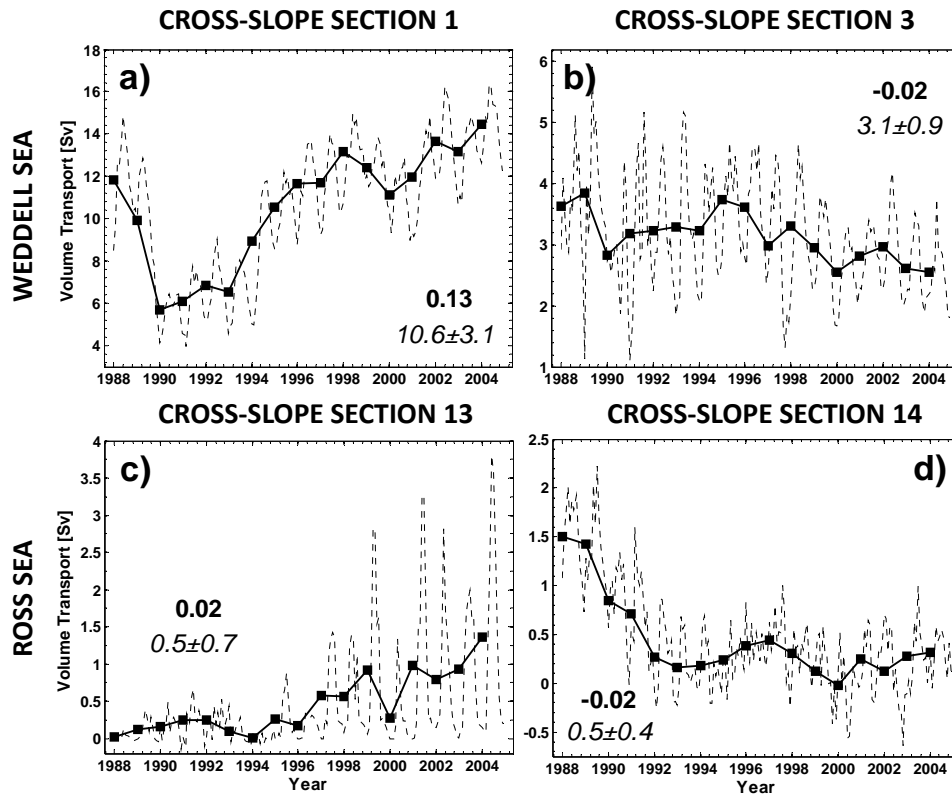


Fig. 8. Monthly (dashed line) and annual (solid line) average of OCCAM-simulated bottom-layer volume transport for (a and b) Weddell and (c and d) Ross Seas cross-slope sections as indicated. The bold and italic annotations show respectively the decadal linear trend (Sv decade⁻¹) and the average and standard deviation for the entire period.

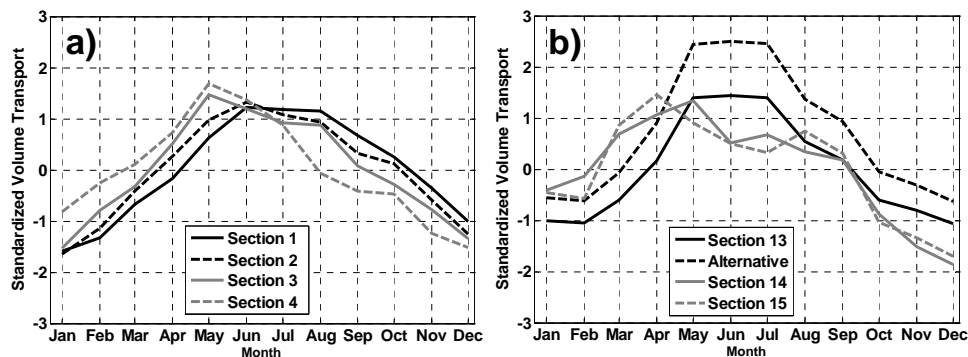


Fig. 9. Standardized annual cycle of the bottom-layer volume transport for the entire OCCAM simulation in (a) Weddell and (b) Ross Seas cross-slope sections as indicated. The units are point-wise normalized and represent the number of standard deviations from the overall mean.

interannual variability at a 3–4 yr period in the Weddell Sea. They pointed out that sea ice changes between 1979 and 1998 were associated with a change in the shape and characteristics of the Weddell Gyre around 1990. Our findings of AABW volume transport variability at 2–4 yr period (Fig. 10) are in consonance with the dominant periods of 3–4 yr reported for coupled processes of AABW production in the Weddell Sea (Venegas and Drinkwater, 2001). However,

while the wind over the Weddell Sea shows a periodicity at 2–3 yr (Fig. 11), the same is not true for OCCAM sea ice concentration and sea ice thickness variability, which show only a periodicity at 1 yr (Fig. 12). The lack of interannual sea ice variability can be in part related to the inability of the OCCAM sea ice model to reproduce an adequate sea ice coverage in the Weddell Sea sector. The modelled sea ice showed dramatic changes after 1994 (Fig. 13). This emphasises the

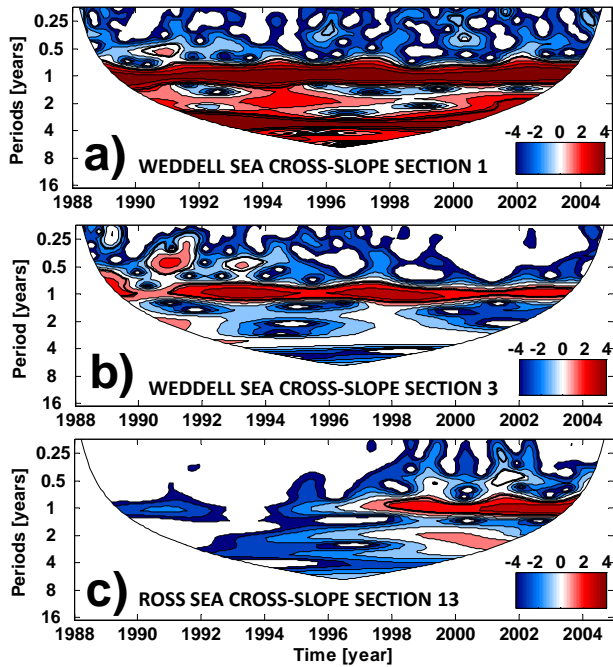


Fig. 10. Wavelet power spectrum of (a) Weddell Sea cross-slope section 1, (b) Weddell Sea cross-slope section 3, (c) and Ross Sea cross-slope section 13 volume transport anomaly using the Morlet wavelet. The white area is the cone of influence, where zero padding has reduced the variance. The black thick contour encloses regions where confidence levels were greater than 90 % for a red-noise process with a lag-1 coefficient of 0.72. The units (colourbar) are the energy in \log_2 form.

role of the correct representation of sea ice formation and melting in models used to understand the physical processes causing AABW variability.

5.3 AABW cross-shelf-break volume transport

The OCCAM bottom-layer mean transport in the north-western Weddell Sea (i.e. across section I in Fig. 1b) is -1.6 ± 1.1 Sv (Fig. 14a), with negative transport denoting eastward flow (offshore). AABW production rates in this region are highly variable with bottom water formation occurring in pulses (Schröder et al., 2002). This occurs in OCCAM also, interspersed with periods of almost total interruption of the spilling process (i.e. 1990–1994 and 2000–2001; Fig. 14a). Pulses of AABW production are observed in OCCAM with average transport varying from 2 to 3 Sv during 1988–1989, 1995–1999, and 2002–2004 (Fig. 14a). Regionally, the main AABW injection into deep layers of the Weddell Sea occurs primarily through the submarine canyons Yelcho and Aurora, with an AABW downslope flow of about 1.5 Sv (Fig. 14b and c).

Orsi et al. (1999) used CFC-11 analysis to show that the circumpolar bottom water production rate ($\gamma'' \geq 28.27 \text{ kg m}^{-3}$) is ~ 10 Sv, which was later supported by

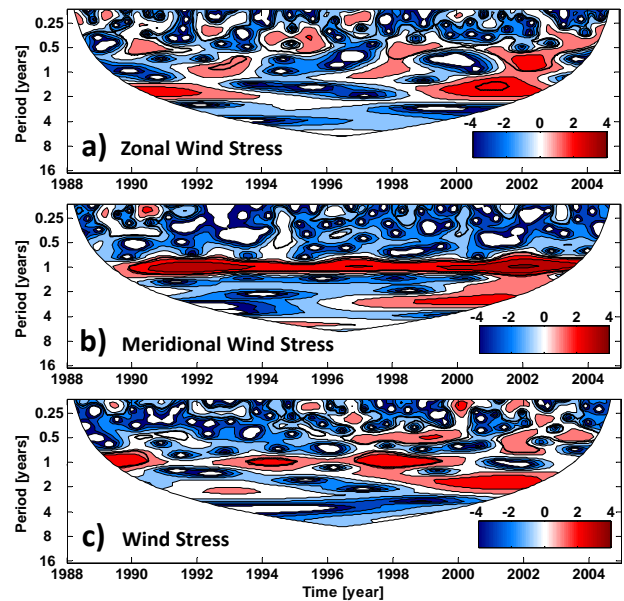


Fig. 11. The wavelet power spectrum of Weddell Sea sector (a) zonal wind stress, (b) meridional wind stress, (c) and wind stress time series using the Morlet wavelet. The white area is the cone of influence, where zero padding has reduced the variance. The black thick contour encloses regions where confidence levels were greater than 90 % for a red-noise process with a lag-1 coefficient of 0.72. The units (colourbar) are the energy in \log_2 form.

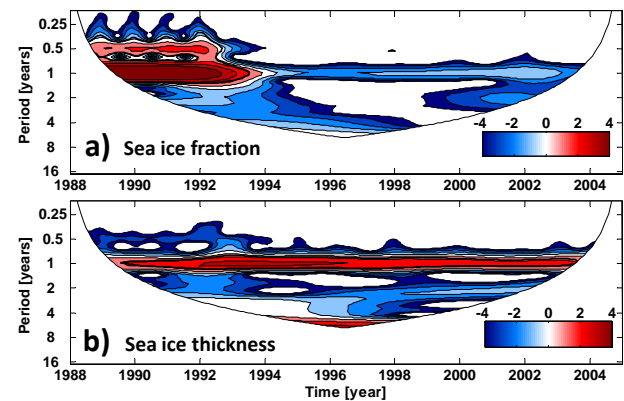


Fig. 12. The wavelet power spectrum of Weddell Sea sector (a) sea ice fraction and (b) sea ice thickness time series using the Morlet wavelet. The white area is the cone of influence, where zero padding has reduced the variance. The black thick contour encloses regions where confidence levels were greater than 90 % for a red-noise process with a lag-1 coefficient of 0.72. The units (colourbar) are the energy in \log_2 form.

Hellmer and Beckmann (2001) through numerical model results. However, Hellmer and Beckmann highlighted that the rate could be doubled if the lighter AABW from the Indian Ocean and Pacific Ocean sectors had been included in their analysis. The bottom water production rate in the Weddell

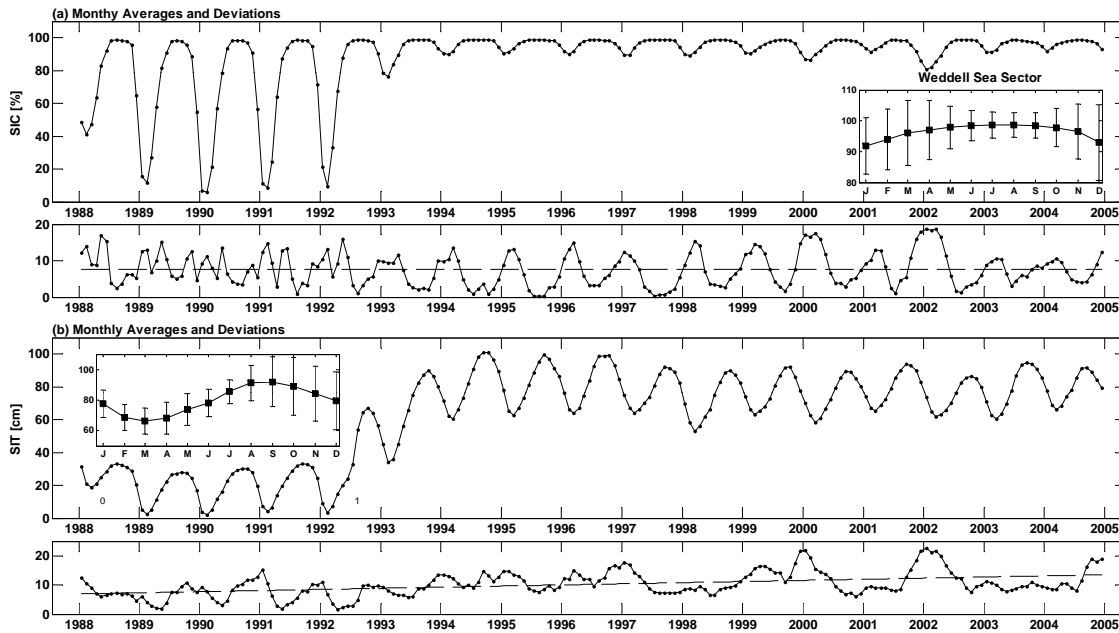


Fig. 13. OCCAM time series of monthly averages of (a) sea ice concentration (SIC) and (b) sea ice thickness (SIT) for the Weddell Sea sector from January 1988 through December 2004. The inset shows the annual cycle computed from the 17 years simulated. The lower panels in (a) and (b) show the monthly deviations of SIC and SIT, respectively, fitted with a linear least-squares best-fit trend line.

Sea according to several observational studies compiled by Orsi et al. (1999) varies from 2 to 5 Sv. They reported a newly formed AABW rate of 4.9 Sv based on their CFC-11 estimates. More recently, Huhn et al. (2008) estimated a bottom water ($\theta \leq -0.7^\circ\text{C}$) formation rate in the western Weddell Sea of 1.1 ± 0.5 Sv. However, Huhn et al. (2008) used a different definition for their bottom-layer transport to that used here. The model AABW layer used here incorporates not only the denser variety of AABW confined in the Weddell Sea (i.e. Weddell Sea Bottom Water – WSBW), as generally reported by observational studies, but also the less dense variety found in the basin (i.e. Weddell Sea Deep Water – WSDW). Thus, although OCCAM represents reasonably well the variability of AABW production in the Weddell Sea region, the volume transport of the flow is only a fraction ($\sim 40\%$) of the water spilling off the shelf in the Atlantic sector of the Southern Ocean.

In the southern Weddell Sea section (i.e. section II in Fig. 1b), the lack of ice shelves in the model prevents the formation of ice shelf water (ISW) onshore, an essential component of AABW in the real ocean (Nicholls et al., 2009). Foldvik et al. (2004) reported an ISW outflow rate about 1.6 ± 0.5 Sv leaving the continental shelf through the Filchner Depression, which implies a rate of WSBW formation of 4.3 ± 1.4 Sv. Matsumura and Hasumi (2010) used high resolution numerical experiments to show a WSBW production rate of ~ 0.15 Sv as a result of descending ISW in this region. Across section II the AABW production is 0.02 ± 0.09 Sv, but on average there is no dense water outflow near the edge of

the Filchner Depression zone (not shown). Given the lack of ice shelves, canyons and small-scale processes in the global model, this is not surprising.

In the Ross Sea along-shelf-break section (i.e. section VII in Fig. 1b), surprisingly no AABW (according to the definition used here) is injected into the southern limb of the Ross Gyre by the model. The possible cause is due to AABW production occurring further south close to the 500 m isobath and, consequently, exportation through the Cape Adare area. An additional along-shelf-break section in the southwestern Ross Sea coastal region gave a bottom water volume transport of 0.31 ± 0.32 Sv. Based on AABW export values reported by Whitworth and Orsi (2006) and Gordon et al. (2009), AABW production in the region should be ~ 2 Sv. Thus, the model reproduced only $\sim 16\%$ of the AABW formation rates expected from observational budgets in the Ross Sea sector.

The volumes of AABW leaving the continental shelf in the Indian Ocean and western Pacific Ocean sectors are also underestimated (< 0.02 Sv). One exception is the AABW crossing Section VI with an average production of 0.2 ± 0.3 Sv. Interannual variability is evident in this offshore flow, with maximum values of 0.4–0.8 Sv during 1994–1997. Since Orsi et al. (1999) determined an AABW production rate of 3.2 Sv when considering both the Indian and Pacific sectors of the Southern Ocean, the total amount simulated by OCCAM represents only $\sim 17\%$ of the total AABW volume expected from the observed CFC-11 budget. OCCAM shows no evidence of dense water cascading down the continental

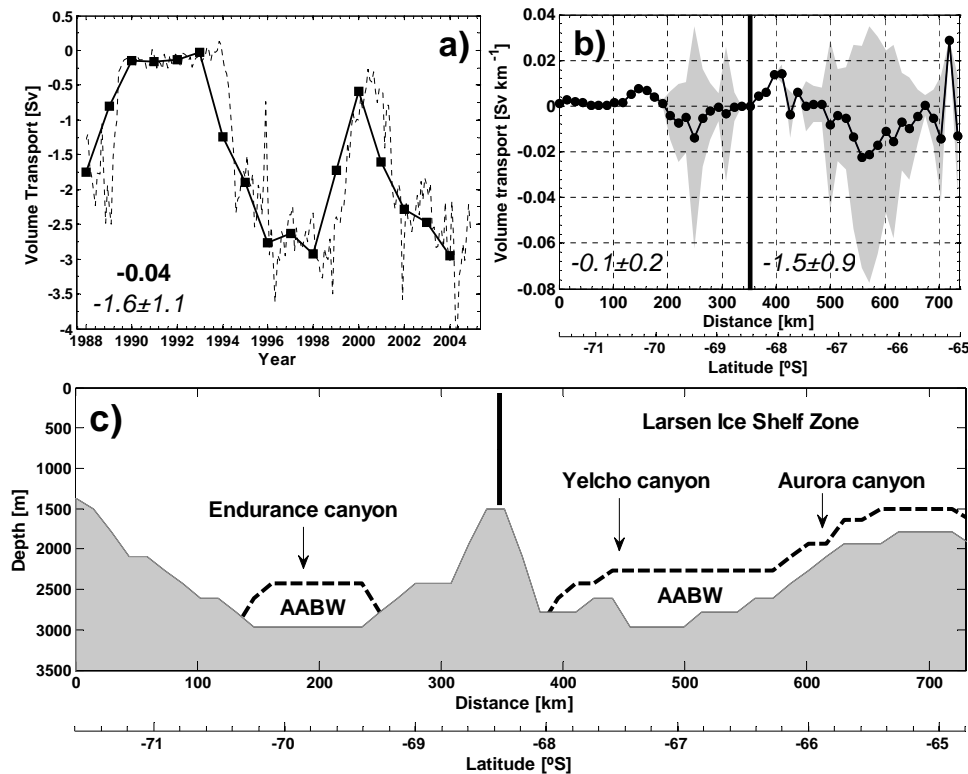


Fig. 14. (a) Monthly (dotted line) and annual (solid line) mean time series of AABW volume transport (in Sv) at northwestern Weddell Sea along-shelf-break section I (see Fig. 1b). The bold and italic annotations show respectively the decadal linear trend (Sv decade^{-1}) and the average and standard deviation for the entire period. (b) Same as described in (a), but vertically integrated and divided by the distance between the model grid points (Sv km^{-1}). The italic annotations show the average and standard deviation for the zone delimited by the black line. (c) Model bathymetry along the section I with the position of the main submarine canyons indicated. The mean AABW layer flowing into the Weddell Sea is indicated by the dashed line.

slope in the B&A Seas sector. This absence agrees with the observations of Baines and Condie (1998), who classified these sectors as null margins of AABW downslope flow (cross-slope sections 17 to 20; Fig. 1a).

The AABW downslope flow around Antarctica often occurs in regions of submarine canyons. In OCCAM this is seen only in the along-shelf-break section of the northwestern Weddell Sea (Fig. 14). It is well known that the shape of the ocean floor and, especially, the seabed corrugations act to steer the main shelf-slope exchange of waters towards the deep ocean, therefore contributing directly to the AABW total flow. Muench et al. (2009) recently highlighted the importance of small-scale local topography when modelling dense outflows in the northwestern Ross Sea. For instance, corrugations enhance entrainment and reduce the along-slope speed of the dense outflow. The bathymetry used in OCCAM was not derived from recent high resolution swath bathymetric surveys around the Antarctic; therefore, it may be locally incorrect and/or too smooth in some regions, which can affect the correct representation of AABW downslope flow.

Export of deep and bottom water from the Ross Sea is particularly sensitive to tides (Padman et al., 2009), but unfortunately tides are not included in OCCAM. Furthermore, z -coordinate models have difficulty in simulating the downslope flow of dense water over continental slope (Wang et al., 2008); these processes are better simulated in sigma coordinate or finite element models. A simple transport budget of AABW flow indicates that bottom waters spilling off the shelf do not contribute enough to the rates of AABW formation in the model; however, some regional areas are still contributing to bottom water production. One of the possible mechanisms to form AABW is open ocean deep convection. During this process, heat losses to the atmosphere in areas of open water cause vertical mixing to depths much deeper than usual. Once initiated, the mixing of warm and salty intermediate water (e.g. WDW, CDW) into the surface layer (generally colder and fresh due to sea ice and atmosphere interactions) brings heat to the surface that can melt sea ice allowing further contact between ocean surface and the atmosphere. This process occurs in open ocean polynyas and is likely to be the process by which ocean/climate models

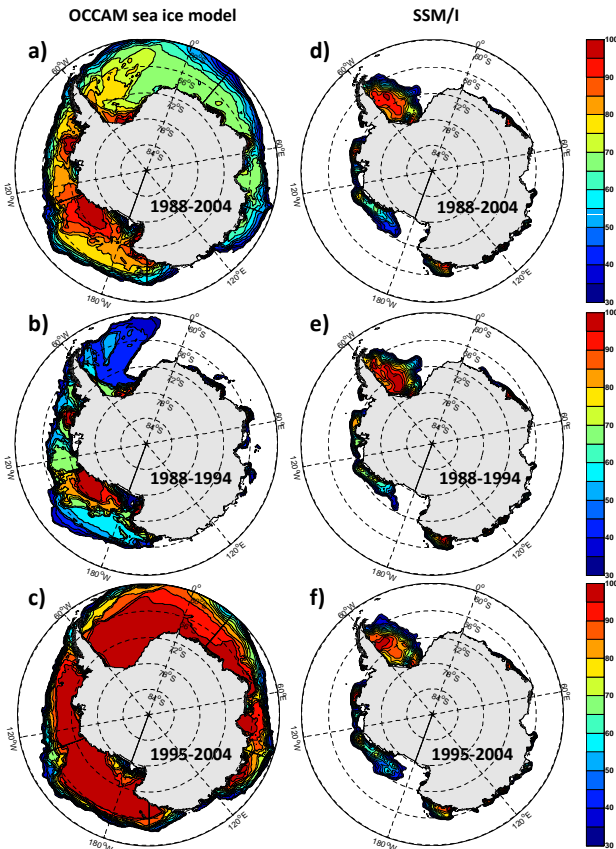


Fig. 15. Climatology of OCCAM (left) and SSM/I (right; from the *National Snow and Ice Data Center*) sea ice concentration (%) during February: (a, d) 1988–2004, (b, e) 1988–1994, and (c, f) 1995–2004.

form large quantities of dense water. Further investigation is needed to clarify the processes of replenishment of AABW in OCCAM, especially after 1994 when the sea-ice simulation becomes unrealistic (Figs. 13 and 15).

We consider now only the AABW volume transport flowing along the continental slope of the main AABW export regions to the global ocean (i.e. the cross-slope sections 1, 9, 10, 13 and 14; Fig. 1a). In OCCAM 8.3 Sv (70%) of AABW exits the Weddell Sea sector through the cross-slope section 1 (i.e. northwestern Weddell Sea; Fig. 16). Considering the other export zones, we found that 3.0 Sv (25.5%) exits the Indian and western Pacific Ocean sector through cross-slope sections 9 and 10, and 0.5 Sv (4.5%) leaves the Ross Sea through cross-slope sections 13 and 14. These results are similar to those of Orsi et al. (1999), who found that 60% of AABW originated in the Atlantic sector and 40% in the Indian and Pacific sectors of the Southern Ocean. Thus, although OCCAM does not properly produce AABW at its formation sites on the continental shelf, it does export AABW at reasonable rates to the global ocean.

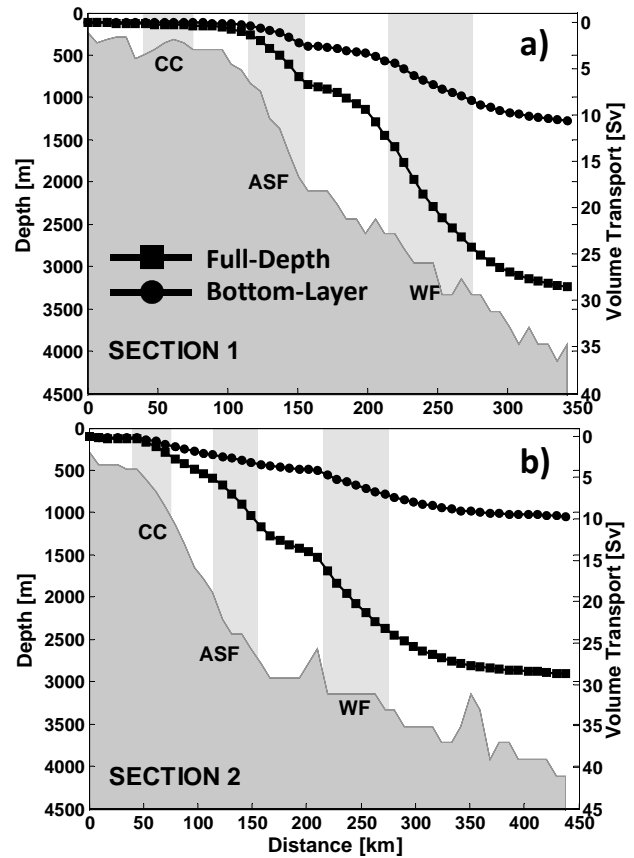


Fig. 16. Mean OCCAM model full-depth (square) and bottom-layer (circle) cumulative volume transport for (a) section 1 and (b) section 2 in the northwestern Weddell Sea. The grey rectangles indicating the zone of the Antarctic Coastal Current (CC), Antarctic Slope Front (ASF) and Weddell Front (WF) as presented by Thompson and Heywood (2008).

6 Correlations between AABW source properties and deep ocean export

Cross-correlation maps between the anomaly time series of the bottom water volume transport and the properties of the AABW source layers were constructed for the four selected model cross-slope sections. Prior to the analyses, a linear trend was removed from each time series, because such trends are likely to be due to model drift. The seasonal cycle was removed from each time series by subtracting monthly means from the data to allow us to see the underlying variability. Finally, we filtered all time series with a Butterworth filter with a 12-month window to further smooth the deseasoned time series. In order to test the robustness of the results obtained, sensitivity analysis (not shown) was performed on different selected SL and IL from the OCCAM model, but changes in the correlation patterns were not significant.

We might expect cold and salty shelf waters to be positively correlated with bottom water export at some lag, if

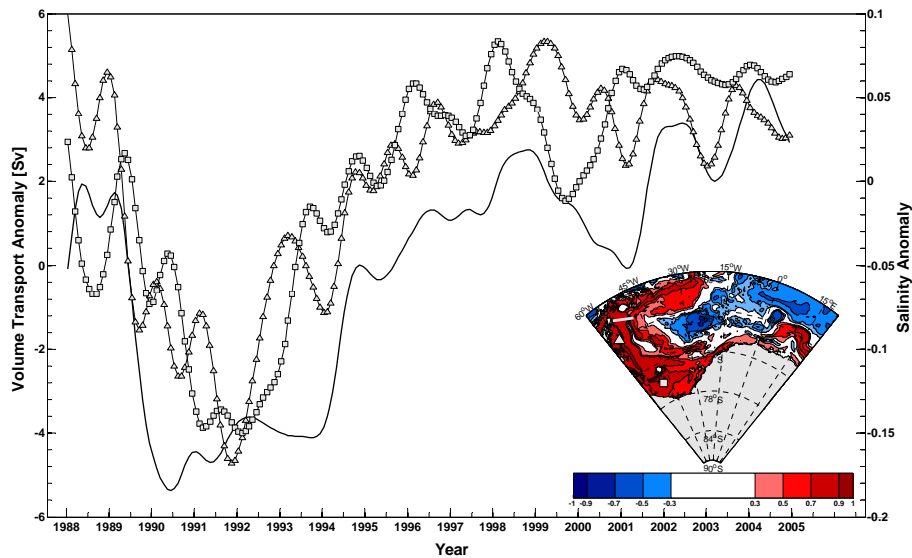


Fig. 17. Bottom-layer volume transport anomaly time series (Sv; black line) of Weddell cross-slope section 1 (inset figure – grey line) and salinity anomaly time series at the locations marked by square and triangle symbols in the inset figure (see caption of Fig. 18), which shows the high degree of correlation between the time series.

we hypothesise that brine is rejected into the lower layers during coastal sea ice formation to make dense shelf waters more abundant over the shelf, which would lead to a greater amount of those dense waters spilling off the continental shelf and thus intensifying AABW formation. Although this might be the case in the real ocean, we do not expect this to be the case in OCCAM, because the model deficiencies previously discussed (e.g. coastal resolution, bottom bathymetry and lack of tides) preclude the model from realistically reproducing the spilling of dense water off the shelf.

The bottom-layer volume transport in the Weddell Sea cross-slope section 1 is significantly correlated ($r \geq 0.7$, $p < 0.05$, $N = 204$) with SL salinity in the Western and Southern Weddell Sea continental shelf (Figs. 17 and 18). All cross-correlations presented highest values at zero lag, which implies that the time series are both responding to the same forcing. We conclude that the Weddell Sea bottom water outflow and circumpolar thermohaline shelf water properties co-vary (Fig. 18). Assuming the OCCAM mean AABW velocities for the whole simulated period to be 4 cm s^{-1} and 1.2 cm s^{-1} for Weddell Sea cross-slope sections 1 and 3, respectively, and a total distance between those sections of about 1515 km, AABW sourced in the southern Weddell Sea will take approximately 1.8 yr to reach the export region. Thus, the high positive correlations between shelf water salinity and bottom water export cannot be taken as cause-consequence, but instead they are co-varying in time, because both are associated with wind forcing, through spinning up or slowing down the Weddell Gyre, mixing the water column and increasing the latent heat flux.

In fact, the high correlation between the AABW outflow and the shelf regime practically disappears when the time series are lagged up to a period of 5 yr (volume transport lagging water mass properties; Fig. 19c). The time interval of 5 yr is consistent with the shelf water residence time of ~ 6 yr reported in the Weddell Sea (Schlosser et al., 1991; Mensch et al., 1998). At this lag shelf water properties are anti-correlated ($r \leq -0.7$; $p < 0.05$; $N = 204$) with bottom water transport at the AABW export zone. Positive high correlations between bottom water transport and SL salinity are found along the western and southern Weddell Sea continental slope and in the CDW inflow region around 20° W (Fig. 19c). The θ field presents a similar pattern of correlation but not as well defined (Figs. 18a and 19a), thus highlighting that the wind is probably driving the variability of both the AABW source properties and AABW export.

The correlation maps between SL thermohaline properties and the bottom water transport at the export section in the Ross Sea showed similar patterns to those of the Weddell Sea at zero lag (Fig. 18a and c). In contrast to the Weddell Sea, AABW with sources within the Ross Gyre will take only 6.5 months to reach the export region near Cape Adare, assuming mean AABW velocities for the whole OCCAM period to be 5.3 cm s^{-1} and 0.7 cm s^{-1} respectively for the Ross Sea cross-slope sections 13 and 14, and a total distance between them of 515 km. The residence time of ~ 4 yr for Ross Sea shelf waters (Trumbore et al., 1991) suggests that it may take several years for the thermohaline variability in shelf water to affect bottom water export.

Correlations between bottom-layer volume transports of cross-slope sections 1 and 3 for the Weddell Sea sector and cross-slope sections 13 and 14 for the Ross Sea sector reach

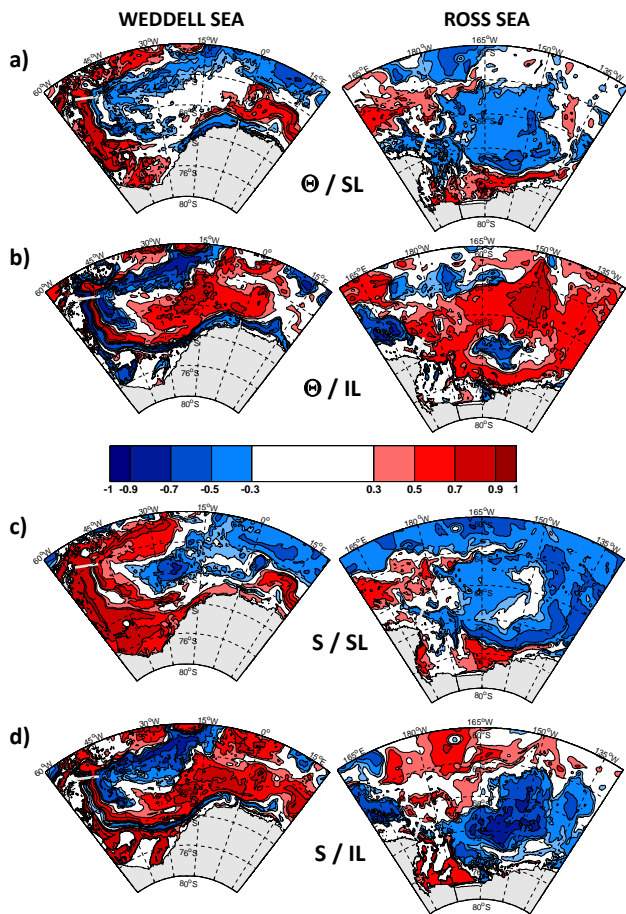


Fig. 18. Cross-correlation maps between model monthly mean bottom-layer volume transport at Weddell and Ross Seas cross-slope sections 1 and 13 (grey line), respectively, onto (a and b) potential temperature and (c and d) salinity at (a and c) SL depth and (b and d) IL depth. All correlations are calculated for zero lag. Only correlation coefficients at 95 % significance level are shown.

their maximum ($r = 0.5$; $p < 0.05$; $N = 204$) at 4.6 yr, which is longer than the calculated transit time for the Weddell (1.8 yr) and Ross Seas (6.5 months). Despite the large uncertainties associated with the estimated advective timescale, future model experiments using virtual tracers/particles could provide better estimates of this variable. In fact, AABW export from those areas has significant contributions from the northwestern Weddell Sea continental shelf bordering the eastern margins of the Antarctic Peninsula (Huhn et al., 2008) and the southwestern area in the vicinity of the Ross Ice Shelf (Whitworth and Orsi, 2006). The time series of bottom water sourced in the northwestern Weddell Sea (Fig. 1b) and exported from the Weddell Sea cross-slope section 1 are highly correlated ($r = 0.8$; $p < 0.05$; $N = 204$) with a time lag of 1 yr, a period consistent with the shelf water residence time recently reported in this region (Hellmer et al., 2011).

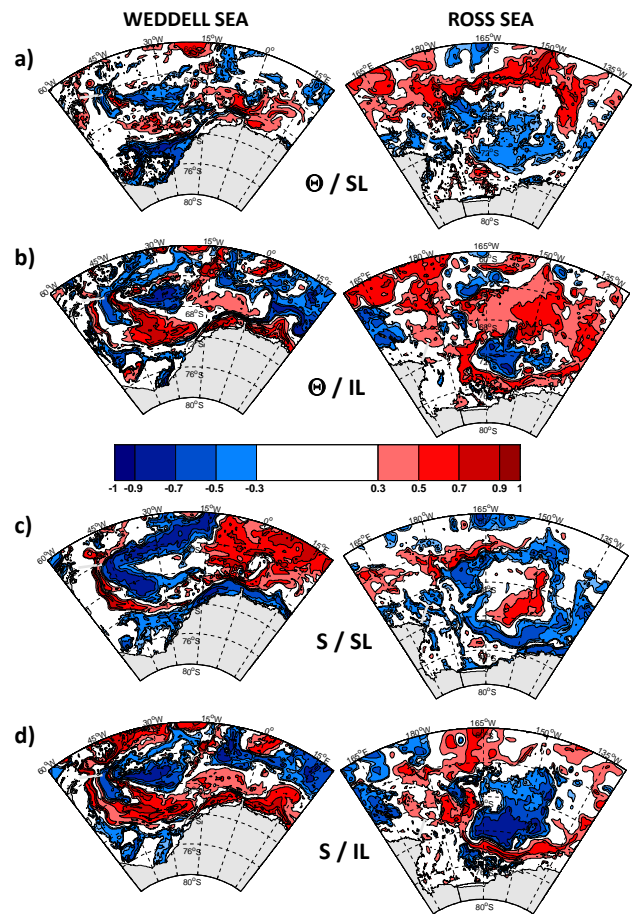


Fig. 19. Same as Fig. 18, but for correlations calculated for lag of five years.

The correlation maps between bottom-layer volume transport and IL properties time series are slightly different from each other (Fig. 18b and d). AABW outflow from the Weddell Sea is correlated ($r \geq 0.5$; $p < 0.05$; $N = 204$) at zero lag with WDW thermohaline properties entering and following the Weddell Gyre circulation. Significant correlations ($r \geq 0.7$; $p < 0.05$; $N = 204$) are found with IL waters at the western Weddell Sea continental slope. In general, bottom water export from the Weddell Sea is significantly correlated with both CDW and WDW characteristics (Fig. 18b and d). High correlation is observed with salinity variability in the deepest areas of the western and southern continental shelves (i.e. densest shelf water variety) of both the Weddell and Ross Seas (Fig. 18d). Once more, correlation at zero lag is likely due to changes in both the export and the inflowing water mass properties being driven by the wind field. Unlike the cross-correlation maps for the SL, for the IL the strongest correlations at zero lag (Fig. 18b and d) are also obtained in the maps at 5 months lag, such as at the western and southern Weddell Sea continental margins (Fig. 19b and d). In fact, 5 yr is approximately the residence time of the waters

(~ 6 yr; Hoppema et al., 2010) in the Weddell Gyre. Dellnitz et al. (2009), through numerical simulation, found that the Weddell Gyre surface and bottom water residence times vary between 1 and 5 yr, while the residence time for intermediate depth water varies seasonally with periods between 5 and 12 yr.

Similar patterns of correlations appear for the IL for both the Weddell and Ross Seas export sections (Fig. 18b and d). In the Ross Sea, the pattern is characterised by positive correlations with CDW properties along the cyclonic gyre circulation and with IL salinity (depth of ~ 500 m) in the Ross Sea coastal regime. However, in the Ross Sea the influence of CDW salinity characterised by positive correlations along the gyre circulation is not as clear at zero lag as in the Weddell Sea (Fig. 18d), but instead the correlation increases as the time series are lagged up to 5 yr (Fig. 19d).

7 Conclusions

In this study, we have shown that OCCAM simulates an average AABW (i.e. $\gamma^n \geq 28.27 \text{ kg m}^{-3}$) outflow of ~ 11 Sv from the northwestern Weddell Sea and only ~ 1 Sv from the Ross Sea. Those rates of AABW export from both regions are in good agreement with observations. The AABW export varies mainly on seasonal and 2–4 yr time scales. In the Weddell Sea, the 2–4 yr period is consistent with the time scale of observed changes in the atmosphere, sea ice, and ocean surface (Venegas and Drinkwater, 2001), which are directly linked to the processes of AABW formation. AABW formed in the southern Weddell Sea will take ~ 2 yr to reach the main export region along the South Scotia Ridge. Thus, those source waters are subject to transformation through mixing with other regional varieties along the path. Furthermore, changes in the thermohaline properties of newly-formed AABW may eventually influence the characteristics of the waters being exported from the Weddell Sea. AABW export co-varies with AABW source water masses thermohaline properties at zero lag, indicating that they are both responding to the wind patterns driving the cyclonic gyre. However, the results cannot be interpreted as cause-consequence, implying that more efforts must be directed to better understand the role of the recent freshening and/or warming trends of AABW sources on changes in AABW production and export to the global oceans.

Data assimilation products, such as the Simple Ocean Data Assimilation reanalysis, have been recently shown to improve the representation of Southern Ocean bottom waters (Kerr et al., 2012), often poorly represented in models (Kerr et al., 2009b). The inclusion of ice shelf processes and other cryosphere components would certainly improve the representation of the water masses at the shelf-break in future simulations, providing a better representation of bottom water properties cascading down the slope to the deep sea. OCCAM shows that an incorrect representation of AABW for-

mation processes near the continental shelf-break does not necessarily imply that the model will not export enough AABW to the global ocean. The proportion of AABW volume injected into the South Atlantic, South Pacific and Indian Ocean Basins is consistent with the observed proportion. Finally, long-term observational studies (and long models simulations) of AABW export and thermohaline properties have to be continued in key areas of AABW outflow, such as the northwestern Weddell and Ross Seas investigated here, but also the region around the Kerguelen Plateau in the Davis Sea as recently indicated by Fukamachi et al. (2010). Models such as OCCAM are useful to increase our understanding of the variability of AABW regional outflows.

Acknowledgements. This study is a contribution to International Polar Year – SASSI (UK) and SOS-CLIMATE (Brazil) projects through the activities of the Brazilian High Latitudes Oceanography Group (GOAL) in the Brazilian Antarctic Program (PROANTAR). GOAL has been funded by the Brazilian Ministry of the Environment (MMA), the Brazilian Ministry of Science, Technology and Innovation (MCTI), and the Council for Research and Scientific Development of Brazil (CNPq; 550370/2002-1; 520189/2006-0). The authors also thank the Brazilian National Institute of Science and Technology of Cryosphere (INCT-CRIOSFERA; 573720/2008-8). R. Kerr acknowledges financial support received from POGO-SCOR Fellowship Program, CNPq PhD Split Fellowship Program (SWE – 201843/2008-0), and CAPES Foundation. Two anonymous reviewers are acknowledged for their constructive comments, which greatly improved the manuscript.

Edited by: G. Williams

References

- Aksenov, Y.: The sea ice-ocean global coupled ARCICE project report part 1: description of dynamical-thermodynamical sea ice model, SOC research & Consultancy Report, 83 pp., Southampton Oceanography Centre, 2002.
- Aoki, S., Rintoul, S. R., Ushio, S., Watanab, S., and Bindoff, N. L.: Freshening of the Adelie Land Bottom Water near 140° E, *Geophys. Res. Lett.*, 32, L23601, doi:10.1029/2005GL024246, 2005.
- Assmann, K. M. and Timmermann, R.: Variability of dense water formation in the Ross Sea, *Ocean Dynam.*, 55, 68–87, doi:10.1007/s10236-004-0106-7, 2005.
- Assmann, K. M., Hellmer, H. H., and Beckmann, A.: Seasonal variation in circulation and water mass distribution on the Ross Sea continental shelf, *Antarctic Science*, 15, 3–11, doi:10.1017/S0954102003001007, 2003.
- Azaneu, M., Kerr, R., Mata, M. M., and Garcia, C. A. E.: Antarctic Bottom Water changes during the last fifty years, *Clivar Exchanges*, 17, 40–43, 2012.
- Baines, P. G. and Condie, S.: Observations and modelling of Antarctic downslope flows: A review, in: *Ocean, Ice, and Atmosphere: Interactions at the Antarctic continental margin*, edited by: Jacobs, S. S. and Weiss, R. F., Antarctic Research Series, 75, Washington DC, AGU, 29–49, 1998.

- Boyer, T. P., Antonov, J. I., Garcia, H. E., Johnson, D. R., Locarnini, R. A., Mishonov, A. V., Pitcher, M. T., Baranova, O. K., and Smolyar, I. V.: World Ocean Database 2005, edited by: Levitus, S., NOAA Atlas NESDIS 60, US Government Printing Office, Washington, DC, 190 pp., 2006.
- Carmack, E. C. and Foster, T. D.: On the flow of water out of the Weddell Sea, *Deep-Sea Res.*, 22, 711–724, 1975.
- Chu, P. C. and Fan, C.: An inverse model for calculation of global volume transport from wind and hydrographic data, *J. Mar. Syst.*, 65, 376–399, 2007.
- Coward, C. A. and de Cuevas, B. A.: The OCCAM 66 Level Model: physics, initial conditions and external forcing. Tech. Rep. SOC Internal Report, No. 99, Southampton Oceanography Centre, 2005.
- DBDB5: US Naval Oceanographic Office, and the U.S. Naval Ocean Research and Development Activity, Digital bathymetric Data Base-5 minute grid, 1983.
- Dellnitz, M., Froyland, G., Horenkamp, C., Padberg-Gehle, K., and Sen Gupta, A.: Seasonal variability of the subpolar gyres in the Southern Ocean: a numerical investigation based on transfer operators, *Nonlin. Processes Geophys.*, 16, 655–663, doi:10.5194/npg-16-655-2009, 2009.
- Fahrbach, E., Rohardt, G., Schröder, M., and Strass, V.: Transport and structure of the Weddell Gyre, *Ann. Geophys.*, 12, 840–855, doi:10.1007/s00585-994-0840-7, 1994.
- Fahrbach, E., Rohardt, G., Scheele, N., Schröder, M., Strass, V., and Wisotzki, A.: Formation and discharge of deep and bottom water in the northwestern Weddell Sea, *J. Mar. Res.*, 53, 515–538, 1995.
- Fahrbach, E., Harms, S., Rohardt, G., Schröder, M., and Woodgate, R. A.: Flow of bottom water in the northwestern Weddell Sea, *J. Geophys. Res.*, 106, 2761–2778, 2001.
- Fahrbach, E., Hoppema, M., Rohardt, G., Schröder, M., and Wisotzki, A.: Decadal-scale variations of water mass properties in the deep Weddell Sea, *Ocean Dynam.*, 54, 77–91, 2004.
- Foldvik, A., Gammelsrød, T., and Törresen, T.: Circulation and water masses on the southern Weddell Sea shelf, in: *Oceanology of the Antarctic Continental Shelf*, edited by: Jacobs, S. S. and Weiss, R. F., Antarctic Research Series, 43, Washington DC, AGU, 5–20, 1985.
- Foldvik, A., Gammelsrød, T., Østerhus, S., Fahrbach, E., Rohardt, G., Schröder, M., Nicholls, K. W., Padman, L., and Woodgate, R. A.: Ice shelf water overflow and bottom water formation in the southern Weddell Sea, *J. Geophys. Res.*, 109, C02015, doi:10.1029/2003JC002008, 2004.
- Foster, T. D. and Carmack, E. C.: Antarctic bottom water formation in the Weddell Sea, in: *Polar oceans*, edited by: Dunbar, M. J., Montreal: Arctic Institute of North America, 167–177, 1977.
- Franco, B. C., Mata, M. M., Piola, A., and Garcia, C. A. E.: Northwestern Weddell Sea deep outflow into the Scotia Sea during the austral summers of 2000 and 2001 estimated by inverse methods, *Deep-Sea Res. I*, 54, 1815–1840, 2007.
- Fukamachi, Y., Rintoul, S. R., Church, J. A., Aoki, S., Sokolov, S., Rosenberg, M. A., and Wakatsuchi, M.: Strong export of Antarctic Bottom Water east of the Kerguelen plateau, *Nature Geosci.*, 3, 327–331, doi:10.1038/NCEO842, 2010.
- Gill, A. E.: Circulation and bottom water production in the Weddell Sea, *Deep-Sea Res.*, 20, 111–140, 1973.
- Gille, S. T.: Warming of the Southern Ocean since the 1950s, *Science*, 295, 1275–1277, 2002.
- Gordon, A. L.: Weddell Deep Water variability, *J. Mar. Res.*, 40(Suppl.), 199–217, 1982.
- Gordon, A. L., Zambianchi, E., Orsi, A., Visbeck, M., Giulivi, C. F., Whitworth III, T., and Spezie, G.: Energetic plumes over the western Ross Sea continental slope, *Geophys. Res. Lett.*, 31, L21302, doi:10.1029/2004GL020785, 2004.
- Gordon, A. L., Orsi, A. H., Muench, R., Huber, B. A., Zambianchi, E., and Visbeck, M.: Western Ross Sea continental slope gravity currents, *Deep-Sea Res. II*, 56, 796–817, doi:10.1016/j.dsr2.2008.10.037, 2009.
- Gordon, A. L., Huber, B. A., Mckee, D., and Visbeck, M.: A seasonal cycle in the export of bottom water from the Weddell Sea, *Nature Geosci.*, 3, 551–556, 2010.
- Gouretski, V. V. and Jancke, K.: A new hydrographic data set for the South Pacific: synthesis of WOCE and historical data. WHP SAC Technical Report No. 2, WOCE Report No. 143/96 (unpublished manuscript), WHP Special Analysis Centre, 1996.
- Hall, A. and Visbeck, M.: Synchronous variability in the Southern Hemisphere atmosphere, sea ice, and ocean resulting from the annular mode, *J. Climate*, 15, 3043–3057, 2002.
- Hay, W. W.: The role of polar deep water formation in global climate change, *Annu. Rev. Earth Planet. Sci.*, 21, 227–254, 1993.
- Hellmer, H. H. and Beckmann, A.: The Southern Ocean: A ventilation contributor with multiple sources, *Geophys. Res. Lett.*, 28, 2927–2930, 2001.
- Hellmer, H. H., Kauker, F., and Timmermann, R.: Weddell Sea anomalies: Excitation, propagation, and possible consequences, *Geophys. Res. Lett.*, 36, L12605, doi:10.1029/2009GL038407, 2009.
- Hellmer, H. H., Huhn, O., Gomis, D., and Timmermann, R.: On the freshening of the northwestern Weddell Sea continental shelf, *Ocean Sci.*, 7, 305–316, doi:10.5194/os-7-305-2011, 2011.
- Hoppema, M., Dehairs, F., Navez, J., Monnin, C., Jeandel, C., Fahrbach, E., and de Baar, H. J. W.: Distribution of barium in the Weddell Gyre: Impact of circulation and biogeochemical processes, *Mar. Chem.*, 122, 118–129, doi:10.1016/j.marchem.2010.07.005, 2010.
- Huhn, O., Hellmer, H. H., Rhein, M., Rodehacke, C., Roether, W., Schodlok, M. P., and Schröder, M.: Evidence of deep- and bottom-water formation in the western Weddell Sea, *Deep Sea Res. II*, 55, 1098–1116, 2008.
- Jackett, S. S. and McDougall, T. J.: A neutral density variable for the world's oceans, *J. Phys. Oceanogr.*, 27, 237–263, 1997.
- Jacobs, S. S. and Comiso, J. C.: Sea Ice and Oceanic Processes on the Ross Sea Continental Shelf, *J. Geophys. Res.*, 94, 18195–18211, 1989.
- Jacobs, S. S. and Giulivi, C. F.: Large Multidecadal Salinity Trends near the Pacific–Antarctic Continental Margin, *J. Climate*, 23, 4508–4524, doi:10.1175/2010JCLI3284.1, 2010.
- Jacobs, S. S., Giulivi, C. F., and Mele, P.: Freshening of the Ross Sea during the late 20th century, *Science*, 297, 386–389, 2002.
- Johnson, G.: Recent decadal warming and freshening of Antarctic-derived abyssal waters, in: *Climate Change: Global Risks, Challenges and decisions*, IOP Conf. Series: Earth and Environmental Science, 6, 032006, doi:10.1088/1755-1307/6/3/032006, 2009.
- Jullion, L., Jones, S. C., Naveira Garabato, A. C., and Meredith, M. P.: Wind controlled export of Antarctic Bottom Wa-

- ter from the Weddell Sea, *Geophys. Res. Lett.*, 37, L09609, doi:10.1029/2010GL042822, 2010.
- Kalnay, E., Kanamitsu, M., Kistler, R., Collins, W., Deaven, D., Gandin, L., Iredell, M., Saha, S., White, G., Woolen, J., Zhu, Y., Leetmaa, A., Reynolds, R., Chelliah, M., Ebisuzaki, W., Higgins, W., Janowiak, J., Mo, K. C., Ropelewski, C., Wang, J., Jenne, R., and Joseph, D.: The NCEP/NCAR 40-year reanalysis project, *B. Am. Meteorol. Soc.*, 77, 437–471, 1996.
- Kerr, R., Mata, M. M., and Garcia, C. A. E.: On the temporal variability of the Weddell Sea Deep Water Masses, *Antarctic Sci.*, 21, 383–400, doi:10.1017/S0954102009001990, 2009a.
- Kerr, R., Wainer, I., and Mata, M. M.: Representation of the Weddell Sea Deep Water Masses in the ocean component of the NCAR-CCSM model, *Antarctic Sci.*, 21, 301–312, doi:10.1017/S0954102009001825, 2009b.
- Kerr, R.: Produção e exportação de águas profundas no entorno do continente Antártico, PhD thesis, Universidade Federal do Rio Grande (FURG), 277 pp., 2010.
- Kerr, R., Wainer, I., Mata, M. M., and Garcia, C. A. E.: Quantifying Antarctic deep waters in SODA reanalysis product, *Pesquisa Antártica Brasileira (Brazilian Antarctic Research)*, 5, 47–59, 2012.
- Killworth, P. D.: Mixing on the Weddell Sea continental slope, *Deep Sea Res.*, 24, 427–448, 1977.
- Large, W. G., Danabasoglu, G., Doney, S. C., and McWilliams, J. C.: Sensitivity to surface forcing and boundary layer mixing in a global ocean model: annual-mean climatology, *J. Phys. Oceanogr.*, 27, 2418–2447, 1997.
- Matsumura, Y. and Hasumi, H.: Modeling ice shelf water overflow and bottom water formation in the southern Weddell Sea, *J. Geophys. Res.*, 115, C10033, doi:10.1029/2009JC005841, 2010.
- Mensch, M., Simom, A., and Bayer, R.: Tritium and CFC input functions for the Weddell Sea, *J. Geophys. Res.*, 103, 15923–15937, 1998.
- Meredith, M. P., Gordon, A. L., Naveira Garabato, A. C., Abrahamson, E. P., Huber, B. A., Jullion, L., and Venables, H. J.: Synchronous intensification and warming of Antarctic Bottom Water outflow from the Weddell Gyre, *Geophys. Res. Lett.*, 38, L03603, doi:10.1029/2010GL046265, 2011.
- Muench, R. D. and Gordon, A. L.: Circulation and transport of water along the western Weddell Sea margin, *J. Geophys. Res.*, 100, 18503–18515, 1995.
- Muench, R. D., Wahlin, A. K., Özgökmen, T. M., Hallberg, R., and Padman, L.: Impacts of bottom corrugations on a dense Antarctic outflow: NW Ross Sea, *Geophys. Res. Lett.*, 36, L23607, doi:10.1029/2009GL041347, 2009.
- Naveira Garabato, A. C., McDonagh, E. L., Stevens, D. P., Heywood, K. J., and Sanders, R. J.: On the export of Antarctic Bottom Water from the Weddell Sea, *Deep Sea Res. II*, 49, 4715–4742, 2002.
- Nicholls, K. W., Østerhus, S., Makinson, K., Gammelsrød, T., and Fahrback, E.: Ice-ocean process over the continental shelf of the southern Weddell Sea, *Antarctica: a review, Rev. Geophys.*, 47, RG3003, doi:10.1029/2007RG000250, 2009.
- Orsi, A. H. and Whitworth, T.: Hydrographic Atlas of the World Ocean Circulation Experiment (WOCE) Volume 1: Southern Ocean, Department of Oceanography, Texas A&M University, College Station, Texas, USA Series Edited by Michael Sparrow, Piers Chapman, and John Gould, 2004.
- Orsi, A. H., Nowlin, W. D., and Whitworth, T.: On the circulation and stratification of the Weddell Gyre, *Deep Sea Res. I*, 40, 169–303, 1993.
- Orsi, A. H., Johnson, G. C., and Bullister, J. L.: Circulation, mixing, and production of Antarctic Bottom Water, *Prog. Oceanogr.*, 43, 55–109, 1999.
- Ozaki, H., Obata, H., Naganobu, M., and Gamo, T.: Long-Term Bottom Water Warming in the North Ross Sea, *J. Oceanogr.*, 65, 235–244, 2009.
- Padman, L., Howard, S. L., Orsi, A. H., and Muench, R. D.: Tides of the northwestern Ross Sea and their impact on dense outflows of Antarctic Bottom Water, *Deep Sea Res. II*, 56, 818–834, 2009.
- Reid, J. L.: On the total geostrophic circulation of the Pacific Ocean: flow patterns, tracers, and transports, *Prog. Oceanogr.*, 39, 263–352, 1997.
- Renner, A. H. H., Heywood, K. J. and Thorpe, S. E.: Validation of three global ocean models in the Weddell Sea, *Ocean Modell.*, 30, 1–15 doi:10.1016/j.ocemod.2009.05.007, 2009.
- Rignot, E. and Jacobs, S. S.: Rapid bottom melting widespread near Antarctic ice sheet grounding lines, *Science*, 296, 2020–2023, 2002.
- Rintoul, S.: Rapid freshening of Antarctic Bottom Water formed in the Indian and Pacific oceans, *Geophys. Res. Lett.*, 34, L106606, doi:10.1029/2006GL028550, 2007.
- Robertson, R., Visbeck, M., Gordon, A. L., and Fahrback, E.: Longterm temperature trends in the deep waters of the Weddell Sea, *Deep Sea Res. II*, 49, 4791–4806, 2002.
- Schlosser, P., Bullister, J. L., and Bayer, R.: Studies of deep water formation and circulation in the Weddell Sea using natural and anthropogenic tracers, *Mar. Chem.*, 35, 97–122, 1991.
- Schröder, M., Hellmer, H. H., and Absy, J. M.: On the near bottom variability in the northwestern Weddell Sea, *Deep Sea Res. II*, 49, 4767–4790, 2002.
- Smedsrud, L. H.: Warming of the deep water in the Weddell Sea along the Greenwich meridian: 1977–2001, *Deep Sea Res. I*, 52, 241–258, 2005.
- Smith, W. H. F. and Sandwell, D. T.: Global seafloor topography from satellite altimetry and ship depth soundings, *Science*, 277, 1957–1962, 1997.
- Taylor, K. E.: Summarizing multiple aspects of model performance in a single diagram, *J. Geophys. Res.*, 106, 7183–7192, 2001.
- Thompson, A. F. and Heywood, K. J.: Frontal structure and transport in the northwestern Weddell Sea, *Deep Sea Res. I*, 55, 1229–1251, doi:10.1016/j.dsr.2008.06.001, 2008.
- Trumbore, S., Jacobs, S. S., and Smethie Jr., W.: Chlorofluorocarbon evidence for rapid ventilation of the Ross Sea, *Deep Sea Res.*, 38, 845–870, 1991.
- Venegas, S. A. and Drinkwater, M. R.: Sea ice, atmosphere and upper ocean variability in the Weddell Sea, *Antarctica, J. Geophys. Res.*, 106, 16747–16765, 2001.
- Whitworth III, T. and Orsi, A. H.: Antarctic Bottom Water production and export by tides in the Ross Sea, *Geophys. Res. Lett.*, 33, L12609, doi:10.1029/2006GL026357, 2006.
- Whitworth III, T., Orsi, A. H., Kim, S.-J., Nowlin Jr., W. D., and Locarnini, R. A.: Water masses and mixing near the Antarctic Slope Front, in: *Ocean, Ice, and Atmosphere: Interactions at the Antarctic Continental Margin*, edited by: Jacobs, S. S. and Weiss, R. F., Antarctic Research Series, 75, Washington DC, AGU, 1–27, 1998.

- Wang, Q., Danilov, S., and Schroter, J.: Comparison of overflow simulations on different vertical grids using the Finite Element Ocean circulation Model, *Ocean Modell.*, 20, 313–335, 2008.
- Wong, A. P. S., Bindoff, N. L., and Forbes, A.: Ocean-ice shelf interaction and possible bottom water formation in Prydz Bay, Antarctica, in: *Ocean, Ice, and Atmosphere: Interactions at the Antarctic continental margin*, edited by: Jacobs, S. S. and Weiss, R. F., *Antarc. Res. Ser.*, 75, Washington DC, AGU, 29–49, 1998.
- Yabuki, T. S., Suga, T., Hanawa, K., Matsuoka, K., Kiwada, H., and Watanabe, T.: Possible Source of the Antarctic Bottom Water in the Prydz Bay Region, *J. Oceanogr.*, 62, 649–655, 2006.